MASTER THESIS

COMPUTATIONAL MODEL OF ACTION SELECTION IN PARKINSON'S DISEASE AND THE EFFECT OF DEEP BRAIN STIMULATION

Joan Benet i Bertran

Faculty of Electrical Engineering, Mathematics and Computer Science
Biomedical Signals and Systems Group
Prof.dr.ir. P.H. Veltink

EXAMINATION COMMITTEE
Prof.dr. R.J.A. van Wezel
Dr.ir. T. Heida
Dr.ir. J. le Feber

10th September 2019

UNIVERSITY OF TWENTE.

Preface

This report is the result of the master's assignment of the specialization of Neurotechnology and Biomechatronics of Electrical Engineering in the University of Twente. The project has been developed during 7 months approximately in the Biomedical Signals and Systems which is part of the Faculty of electrical engineering, mathematics and computer science. The thesis is about the development of a computational model of the cortico-basal ganglia-thalamocoritcal loop to see its response when action selection tasks are performed, and later evaluation in Parkinson's disease simulation. Finally, response of the network when treatment with deep brain stimulation is applied is also analyzed.

I would like to express my gratitude to dr.ir. Ciska Heida for its guidance and supervision during the whole project.

Abstract

Parkinson's disease is a neurodegenerative disease characterized by the loss of dopaminergic neurons in the brain which cause tremor, bradykinesia, rigidity, postural instability, and cognitive impairment, among others. This symptomology is present in several tasks, e.g., action selection tasks. These tasks consist in sending a cue to the subject which indicates him to perform a task or withhold its response and do not perform the task. With these tasks what is attempted is to understand the aspects of the disease and work for more efficient treatments, which is also done by means of computational model which try unravel the theoretical aspects of the disease.

In the current thesis, a model of the cortico-basal ganglia-thalamocortical loop is developed to try to reproduce the effects of action selection tasks in Parkinson's disease conditions. The model is based in the Hodgkin-Huxley description of ion channels dynamics of the different populations of neurons that conform this loop with exception of the cortex, which is modeled by means of input/output functions to the other populations. The representation of action selection tasks in the model is used to study if the increase of the β-band (13-30Hz) in the subthalamic nucleus that is seen when these tasks are performed in parkinsonian cases is reduced when proper deep brain stimulation (DBS) is applied and then, to see if this frequency band can be used as biomarker for DBS.

The model shows a good approximation of the network, obtaining the expected behavior of the network in resting conditions and the increase of the β-band as the severity of the disease is increased. With respect to the application of DBS, high frequency and low frequency DBS are applied, showing a decay of the β-band for high frequency DBS and a large increase for low frequency DBS. The results are an indicator that high frequency is an optimal treatment that eliminates the erratic oscillations and it the gives possibility of using the β-band as biomarker for treatment as the decay is noticeable. On the other hand, the increase of the β-band for low frequency DBS might be an indicator of the bad outcome obtained when this treatment has been applied.

Table of contents

Abbreviations

Anterior cingulate cortex (ACC)
Deep brain stimulation (DBS)
Dopamine (DA)
Dorsolateral prefrontal cortex (DLPFC)
Fast spiking interneuron (FSI)
Frontal eye fields (FEF)
γ-aminobutyric acid (GABA)
Globus pallidus externus (GPe)
Globus pallidus internus (GPi)
Local field potential (LFP)
Medium spiny neuron (MSN)
Parkinson's disease (PD)
Prefrontal cortex (PFC)
Pre-sensorimotor area (pre-SMA)
Substantia nigra pars compacta (SNc)
Substantia nigra pars reticulata (SNr)
Subthalamic nucleus (STN)
Supplementary eye fields (SEF)

1. Introduction

Parkinson's disease (PD) is the second most common neurodegenerative disease which is estimated to affect more than 2-3% of people over 65 years of age, rare to see in people below 50 years of age and with a global incidence of 5 to more than 35 new diagnosed cases per 100000 people yearly, estimating a worldwide affected population of 7 to 10 million.[1][2][3] PD has 1.5-2 times more incidence in men than women, despite some studies have shown that in certain populations no difference is observed, and it has no effect in the mortality during the initial decade of the disease, but afterward it doubles its values in comparison to healthy people.[1][4][5]

PD is characterized by the loss of dopaminergic neurons and the accumulation of intracellular proteins, which is a common problem in other neurodegenerative diseases besides PD. Loss of dopaminergic neurons starts in the substantia nigra (located in the basal ganglia) and near regions of the midbrain, spreading to other regions of the brain at more advanced stages of the disease.[6][7] The accumulated protein is α-synuclein, a nuclear protein which forms aggregates like the Lewy bodies in the cytoplasm of neurons in different brain regions.[8] Main symptoms of PD are tremor, bradykinesia, rigidity and postural instability. Besides these, other common symptoms in PD subjects are cognitive impairment, disorders of mood, disorders of sleep-wake cycle regulation and pain.[9][10] Functions related to difficulties in the movement are generated by malfunction of the thalamo-cortico-basal ganglia circuits (Figure 1), which are responsible for the control of actions and goal-directed behavior. These circuits build a loop structure that receives
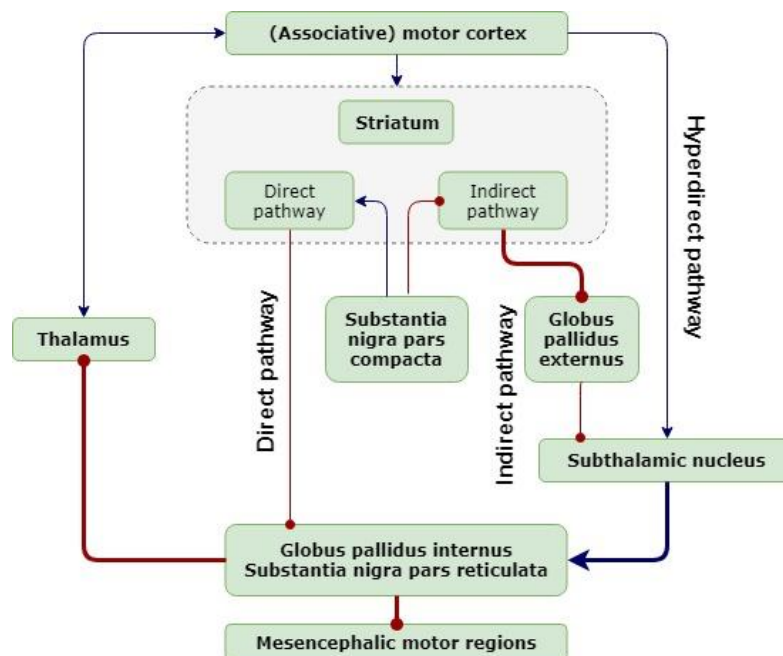
Figure 1. Scheme of the different components of a thalamo-cortico-basal ganglia circuit and how their connections' instensity are affected due to PD. Blue arrows indicate the excitatory connections and red arrows represent the inhibitory connections. Thicker arrows indicate stronger connections with respect to healthy conditions and narrower show decreased intensity of the connections. The three different pathways are indicated for clearer visual differentiation.[1]

signals from the cortex regions of the brain and they converge in a few subcortical regions to give back a response to the cortex.[1][11][12]

As aforementioned, PD results from the reduction of dopaminergic transmission from the substantia nigra pars compacta (SNc), to the striatum, which results in higher inhibition of the thalamus and then, lower activation of the cortex. This inhibition is produced following a set of connections or pathways, having three pathways that can be differentiated: the direct pathway, the indirect pathway, and the hyperdirect pathway.

The direct pathway is a neural pathway in the basal ganglia which involves the cortex, the striatum, the substantia nigra, the globus pallidus internus (GPi) and the thalamus. This pathway facilitates desired movements avoiding the inhibition of the corresponding zones of the GPi and then of the thalamus.[13][14][15] The striatum receives input signals from the cortex which cause its activation together with the SNc, which sends dopamine (DA) to the neurons of the striatum received by the dopamine receptor 1.[16] These activated neurons of the striatum, later on, act on the GPi and the substantia nigra pars reticulata (SNr) inhibiting its activity mainly by means of γ-aminobutyric acid (GABA), what causes that this GPi-SNr complex cannot prolong this inhibition to the thalamus, allowing the proper activation of specific zones of the subject's thalamus and cortex.[16] The death of DA neurons of the SNc causes that less activation of striatum neurons occurs and, subsequently, GPi and SNr have not enough inhibition. GPi and SNr disinhibition lead to higher inhibition of the thalamus, avoiding proper movement in those subjects which have a non-functional direct pathway.[15]

The indirect pathway works complementary to the direct pathway by suppressing the activity of those thalamic regions that are not involved in the corresponding movement.[13][14][15] It has a longer route than the direct pathway, including the cortex, the striatum, the substantia nigra, the globus pallidus externus (GPe), the subthalamic nucleus (STN), the GPi and the thalamus. Equally as in the direct pathway, striatum receives input signals from the cortex and SNc, but in this case, the last one sends inhibitory dopaminergic signals to those neurons as they have the dopamine receptor 2 as target protein. The striatum inhibits the GPe by means of mainly GABAergic transmissions, which also inhibits the STN. The STN acts again on the GPi-SNr causing its activation which can be used to inhibit the regions of the thalamus that do not participate in the action. When there is a loss of dopaminergic neurons in the SNc, a higher activation of the striatum is produced, which triggers a cascade of inappropriate signals, causing a higher inhibition of the GPe and generating higher activation of the STN and also the GPi-SNr. This higher activation of the last complex is converted into more inhibition than the one which corresponds to the thalamus, what can cause the impaired movement symptoms seen in PD.[15]

The final pathway of the thalamo-cortico-basal ganglia circuit is the hyperdirect pathway, which was the last one to be identified and it is a rapid way to send an overall inhibition to the thalamus, supporting the indirect pathway in the inhibition of the thalamic regions which do not have to be activated, and giving more time to the other pathways to resolve conflicts of neural activation.[1][13][14][15][17] This path is constituted by the cortex, the STN, the GPi-SNr and the thalamus. The cortex activates directly the STN, giving a faster response than the one seen in the two previous pathways; and from

the STN on, the route that the signals follow is the same as in the indirect pathway, giving extra time to the other pathways to solve activation conflicts.[13]

However, malfunction of the firing rates of these three pathways is not enough to explain the whole effects of Parkinson. Beta power band (13-30 Hz) has been shown to be the main factor in the problems of bradykinesia observed in Parkinson's subjects.[1] Abnormal synchronization occurs in this frequency band, which leads to hypokinesia as synchronization in the β-band suppresses movement and decrease of this synchronization is seen in healthy subjects prior and during movement.[18] To find the origin of this enhanced β-band activity has become a major goal in the PD study and different sources have been proposed like the cortex, the cerebellum or the basal ganglia.[19][20] STN-GP circuits' ability to generate different patterns of activity under different conditions converted them into important candidates for the origin of this synchronization, or at least showed that they are critically involved.[21]

To the mostly known motor impairment that cause the tremor and bradykinesia problems that cause problems of movement, the cognitive impairment deficiencies are also present in PD and have a big incidence in life of patients. These cognitive problems are seen visible in *Gauggel et al. 2004*, where scores in tests of several cognitive features like vocabulary or spatial thinking are decreased for PD patients and reaction times to execute or inhibit certain actions are increased.[22] The increase in reaction time could be confused with motor deficits, but subjects show that they are capable to perform the task, implying that problems are more related to cognitive problems to fully understand the task they are demanded in the moment, or solve internal conflicts of the brain for inhibition or activation of certain zones. These problems are supported with papers like *Cooper et al. 1994, Pasquearau et al. 2017* and *Benis et al. 2014*, where all show the increase of reaction times in PD.[23][24][25]

A. Computational models

To prove or find how malfunction works in PD, i.e., where is it generated or how abnormal firing rate of one region affects the others, basal ganglia models appeared as a key tool to understand the mechanisms behind the disease. These models are mathematical descriptions of the different parts of a complex system to study its behavior and usually try to explain the results obtained in experimental work. In PD, these models are designed accordingly to what is wanted to study, from simple models of just some basal ganglia's nuclei or the whole cortico-basal ganglia-thalamocortical complex. Besides the nuclei involved in the different models, parameters included in these models also play a crucial role depending on if they might have an influence or not in a specific situation.

An example of a relatively simple model in terms of the number of neuronal populations modeled is the one developed by *Otsuka et al. 2004*. In this model, the STN is the only modeled nucleus as it is done to observe how STN generates plateau potentials and to study the influence of the different ion channels dynamics in the generation of the plateau potentials.[26] Another model that could be considered simply in the same terms is the one developed by *Terman et al. 2002*. This model consists of the generation of Hodgkin-Huxley potentials to represent the STN-GPe loop and study how different

architectures of connection influence the firing patterns, together with which are relevant parameters of the mentioned populations for these patterns.[27] It is stated that the results can be useful to explain the irregularity or rhythmicity of the neurons, which cause the common symptom of tremor visible in PD. Despite the model does not include more compartments than the STN and the GPe, the importance of this loop has caused the replication of this model in several papers where different aspects were studied. In *Sungwoo et al. 2016*, the model is used to study if β-band synchronization is originated in the STN-GPe loop by applying different conditions and evaluating the response.[21] Another example is seen in *Park et al. 2011*, where this same model is used to analyze the temporal structure of the phase-locking and to show that synchronous oscillations are highly influenced by the coupling strength.[28] A similar model to the one designed by *Terman et al. 2002* is the one developed by *Nevado-Holgado et al. 2014*. They modeled the same loop, but unlike the previous, it is a single neuron model which breaks down the GPe in two different kinds of neurons to find if any type of the GPe neuron has different connectivity parameters with the STN, proving the different populations of neurons present in the GPe as the best results were reflected when the populations were unbalanced and had different autonomous firing rates.[29] All these models of the GPe-STN loop have high relevance in the study of PD as the STN is as a relevant actor in PD, being one of the targets for PD treatments, and GPe is one of the main regulators of its activity.[19][30][31]

Another model containing a small loop consisting of by just a few population of neurons is the one of *Corbit et al. 2016*. In this model, the pallidostriatal loop is developed between the GPe and the striatum, which divided into fast-spiking interneurons (FSI) and medium spiny neurons (MSNs), to better describe its behavior during healthy and DA-depleted conditions, showing that the last promotes synchronization and rhythmicity.[32] The relevance of this loop is found in the generation of synchronicity and rhythmicity of the basal ganglia under DA-depleted conditions, becoming an important factor for the problems caused in PD.

Other models with higher number of modeled nuclei also attempted to capture the overall behavior of the whole system, like the one developed by *Rubin et al. 2004*. This is a more complex model of *Terman et al. 2002* model, developed by the same authors but this model contains the direct and indirect pathways, which go from the striatum to the thalamus to try to unravel the mechanisms of deep brain stimulation (DBS) in Parkinson's subjects when applied to the STN, increasing the firing rates and desynchronizing the spikes.[27][33] Finally, several models include the whole compartments in the thalamo-cortico-basal ganglia loop to describe the whole behavior of the system as seen in *Pavlides et al. 2015* and *Baston et al. 2015*. The first model attempts to reproduce the behavior of the whole system and how the variation of the different parameters and connections lead to the behavior seen in PD, to find which pathways or connections are essential for the β-band oscillations.[34] In the second one, the model is designed to analyze how action selection is made in populations of neurons that are part of the cortico-basal ganglia-thalamocoritcal loop, unraveling the role and performance of each of the pathways during this action selection to withhold the

responses while the conflict is solved, along with the behavior of the system during PD and plasticity of the network due to previous solved conflicts.[14]

B. Action selection tasks

These models have contributed to the study of PD and have allowed the understanding of certain aspects of the disease, like the relevance of certain connections or parameters in the generation of the synchronization patterns of the spikes. However, to further understand the pathophysiology of the disease, action selection tasks are designed and performed on subjects (Go/No-Go or Stop tasks), which are useful to evaluate the reaction times and the ability to inhibit signals in PD patients, evaluating not only their motor functions but also their cognitive impairement.

Go/No-Go tasks consist in experiments where the subject receives some kind of stimulus (usually visual or auditory) which has different possible outputs. Subjects are taught to have a certain response in some of the outputs, for example pressing a button, which constitute the Go task, and do not perform the action or withhold its response in the other stimuli, constituting the No-Go task. The procedure followed in these tasks is seen in Figure 2, alternating one kind of response with the other. This kind of task is used in *Cooper et al. 1994*, where healthy and PD patients received a different kind of stimuli of increased complexity to evaluate the differences in reaction time and cognitive function, showing a significantly worse result in PD for both factors.[23] Other examples of Go/No-Go tasks are also used in *Kuhn et al. 2004* and *Pasquearau et al. 2017*, looking at the synchronization of neural activity and reaction times respectively.[18][24]

Another common task used in PD for evaluating reaction tasks and inhibitory ability of subjects is the Stop task. It is similar to the Go/No-Go but a continuous stimulus is usually presented to the participants which have to perform an action while it is presented, until a certain trigger appears and informing the participant to stop doing the task. *Gauggel et al. 2004* uses a Stop task to evaluate the reaction time of Parkinson's patients and their ability of inhibition, obtaining also a worse performance in patients.[22] A more complex Stop task is presented in *Benis et al. 2014*, combining stop signals with warnings that give certain information to the user and the researchers use this study to evaluate not only reaction times, but also β-band amplitude to see how the different warnings have an influence on brain signals.[25]

Computational models and reaction tasks unraveled some questions related with PD and offered a better understanding of the disease. However, the final goal of both of these
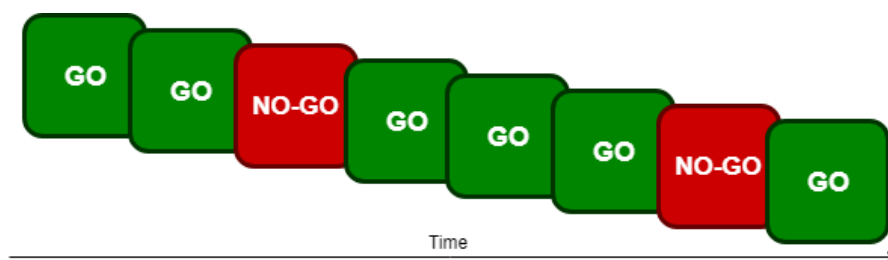

Figure 2. Example of a Go/No-Go task. Go and No-Go stimuli are alternated randomly and the subject has to respond or not according to the stimulus it is receiving in the specific moment.

studies is to find a possible treatment to cure patients or fight its symptoms. Treatment with dopaminergic targets like levodopa is the leading treatment for PD, but the breakthrough of DBS as possible treatment of PD when applied in the STN became a prominent discovery.[1][35] DBS consists in high-frequency electrical stimulation of specific brain targets without destroying brain tissue, but the exact reason of why physiological spike firing patterns are suppressed in the brain is unclear.[31] Moreover, DBS also has a repairing ability in Go/No-Go tasks for PD subjects, avoiding errors in No-Go tasks or freezing episodes in Go tasks, returning the motor and cognitive control to the subjects.

In this thesis, a model of the cortico-basal ganglia-thalamocortical loop is developed to see if changes in terms of synchronization and firing occur in the β-band while a Go/No-Go task is performed by Parkinson's patients. Furthermore, the effect of DBS is studied in patients while the task is performed to find if the STN's β-band can be used as a biomarker during DBS treatment of Parkinson's patients for adaptive control of DBS.

2. Methods

The goal of the thesis was to find out if STN's β-band during performance of action selection tasks like Go/No-Go tasks can be used as biomarker for DBS in PD subjects. To do so, a computational model of the basal ganglia was developed following the Hodgkin-Huxley model of neurons, PD conditions were simulated by modifying the electrophysiological parameters of the different neuronal populations, and the model was analyzed by looking at the response of the neuronal populations. Implementation of the model and the necessary processing steps were both performed in MATLAB (Mathworks, Inc., R2018b). The final statistical analysis of the data was performed in SPSS v23 (SPSS Inc. Chicago, IL, USA).

A. Computational model

As the goal of the assignment was to study the behavior of the brain in PD, the designed regions of the brain were those that are part of the pathways involved in action selection tasks and affected by the characteristic loss of DA produced in PD. This resulted in modeling the following parts: thalamus, GPi, GPe, STN, and Go and No-Go parts of the striatum.

The Hodgkin-Huxley model used in the thesis consists in a set of nonlinear differential equations which describe the electrical features of cell membranes and how the action potentials generated by them are initiated and propagated. The membrane is modeled as a capacitance (C_m) and the ions entering through the different pumps as currents (I_X) as shown in Figure 3. In the current model, the currents used were those which are relevant on each population and allow their firing according to their behavior.

Modifications occurred with respect to the initial model developed by Hodgkin and Huxley in 1952 as new discoveries were performed in the field, describing the behavior of other currents in addition to the leakage, K^+ and Na^+ and the influence of each type of neurons to the other type of populations that are connected. This more complex
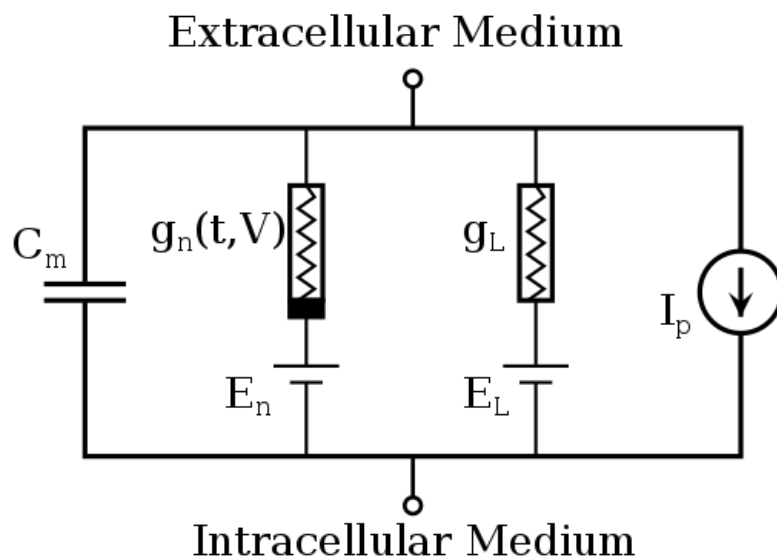

Figure 3. Schematic of the basic Hodgkin-Huxley model of a neuron. Subindex L states for the leakage current and subindex n states for the different ions used in the model of the neuron. As more ions used, more branches corresponding to each ion must be included.

description of the behavior of the neurons is well shown in *Terman et al. 2002* and *Rubin et al. 2004*, which described the loop formed by the STN and GPe in the first article and added the GPi and the thalamus in the second.[27][33] Because of the similarity between the goal of the articles and the goal of the assignment, the same model was used to design the neurons in this assignment (this kind of model has also been used in other models, proving its validity).

The Hodgkin-Huxley model consists in describing the electrical features of cell membranes to see the propagation of their action potentials. The membrane, represented by the C_m, was used to determine the currents going through it and the variation of the currents were used to finally obtain the variation of potential through the membrane. A general description of the modeled neurons is given in Eq. (1), but some variations were applied to each population if necessary.

$$C_m \frac{dV}{dt} = -(I_L + I_K + I_{Na} + I_{Ca} + I_T + I_{AHP} + I_{A \to B}) + I_{App} \tag{1}$$

where dV/dt is the variation of the membrane potential over time, I_L is the leakage current, I_K is the K$^+$ current, I_{Na} is the Na$^+$ current, I_{Ca} is the high threshold Ca^{2+} current, I_T is the low threshold T-type Ca^{2+} current, I_{AHP} is the afterhyperpolarization (AHP) current, $I_{A \to B}$ is the current coming from other neuronal populations, and I_{App} is the current coming from other external sources applied to the neuronal population. Not all the currents were used for all the populations as the firing pattern of the different neurons were different. Which currents were used for each neuron is explained in the following pages in detail.

Each of the currents have their own intrinsic properties, so they were developed according to their characteristics and the number of gating variables and the dependence of them changed on each current. The leakage current was the only current independent of time and voltage, with no gating variables and defined by:

$$I_L = g_L(V - E_L) \tag{2}$$

where g_L is the leakage conductivity and E_L is the rest potential of the leakage current.

The remaining currents had gating variables which changed their state according to the membrane potential (time independent) and in some cases also time. This was the case for the K$^+$ current, the inactivating gating variable of the Na$^+$ current and the inactivating gating variable of the low threshold T-type Ca^{2+} current, which are considered slow activating gating variables and their activation is not instantaneous. The gating variables lead to the following ionic current equations:

$$I_K = g_K n^4 (V - E_K) \tag{3}$$

$$I_{Na} = g_{Na} m_\infty^3 h (V - E_{Na}) \tag{4}$$

$$I_{Ca} = g_{Ca} s_\infty^2 (V - E_{Ca}) \tag{5}$$

$$I_T = g_T a_\infty^3 r(V - E_T) \tag{6}$$

where g_X is the conductivity and E_X is the rest potential of the different ions. The different letters state for the gating variables of each ionic current. Those letters with the infinite subindex indicate the gating variables that did not change as a function of time, but only as a function of the membrane voltage, representing the steady-state of the gates. This steady-state was computed according to:

$$X_\infty = \frac{1}{1 + e^{-(V - \theta_X)/\sigma_X}} \tag{7}$$

where X_∞ is the steady-state of the gate, θ_X is the half activation (or inactivation) potential of the corresponding gating variable, and σ_X is the slope factor of the gating variable. This steady-state was computed for all the gating variables, being used in the mentioned cases as the gate and in the time dependent to calculate the state of the gate at each moment in time.

To the gating variables n, h and r that also depend on time, first-order kinetics functions were defined which captured the variation of the state of the gate over time. Their behavior was described by:

$$\frac{dX}{dt} = \Phi_X \frac{X_\infty - X}{\tau_X} \tag{8}$$

where dX/dt is the variation of the gating variable over time, Φ_X is the time scaling constant which captures the velocity of (in)activation of the gates, X_∞ is the steady-state of the gate, X is the actual state of the gate, and τ_X is the time constant of the gate. The time constants of the gates were neither constant and their behavior changed according to the voltage following:

$$\tau_X = \tau_0 \frac{\tau_1}{1 + e^{-(V - \theta_X^\tau)/\sigma_X^\tau}} \tag{9}$$

where τ_0 and τ_1 are the minimum and maximum time constant respectively, θ_X^τ is the potential at which the time constant is the half between minimum and maximum, and σ_X^τ is the slope factor for the time constant.

The final intrinsic current of Eq. (1) was not governed by the same kind of equation. This I_{AHP} is a calcium-dependent current that is activated when the Ca^{2+} concentration inside the neuron increases. Then, the neurons try to compensate the hyperpolarization of the membrane by opening the K^+ channels. The behavior of such current is:

$$I_{AHP} = g_{AHP}(V - E_{AHP})\left(\frac{[Ca]}{[Ca] + k_1}\right) \tag{10}$$

where g_{AHP} is the conductivity of the AHP current, E_{AHP} is the rest potential of the AHP, [Ca] is the intracellular concentration of Ca^{2+}, and k_1 is the dissociation constant of the calcium involved in the AHP current. [Ca] is changing in time according to:

$$\frac{d[Ca]}{dt} = \epsilon(-I_{Ca} - I_T - k_{Ca}[Ca]) \tag{11}$$

where ϵ is a combination of buffers, cell volume and the molar charge of Ca^{2+}, and k_{Ca} is the Ca^{2+} pump rate constant.

The final current implemented in the model due to the network built was the synaptic current. This synaptic current is an extrinsic input to the cell coming from other populations of neurons, which can activate (glutamatergic activation) or inhibit (GABAergic inhibition) the receiving population. The synaptic current was introduced as:

$$I_{A \to B} = g_{A \to B}(V - E_{A \to B}) \sum s_j \tag{12}$$

where $g_{A \to B}$ is the conductivity from population A to B, $E_{A \to B}$ is the rest potential from population A to B, and s_j is the synaptic variable indicating the influence of every presynaptic neuron from population A to the corresponding postsynaptic neuron of population B. These synaptic variables are governed by first-order differential equations:

$$\frac{ds_j}{dt} = \alpha H_\infty (1 - s_j) - \beta s_j \tag{13}$$

where ds_j/dt is the synaptic variable variation over time, H_∞ is an approximation of the Heaviside step function, and α and β are time constants of the release and decay of neurotransmitters. The approximation of the Heaviside step function was made according to:
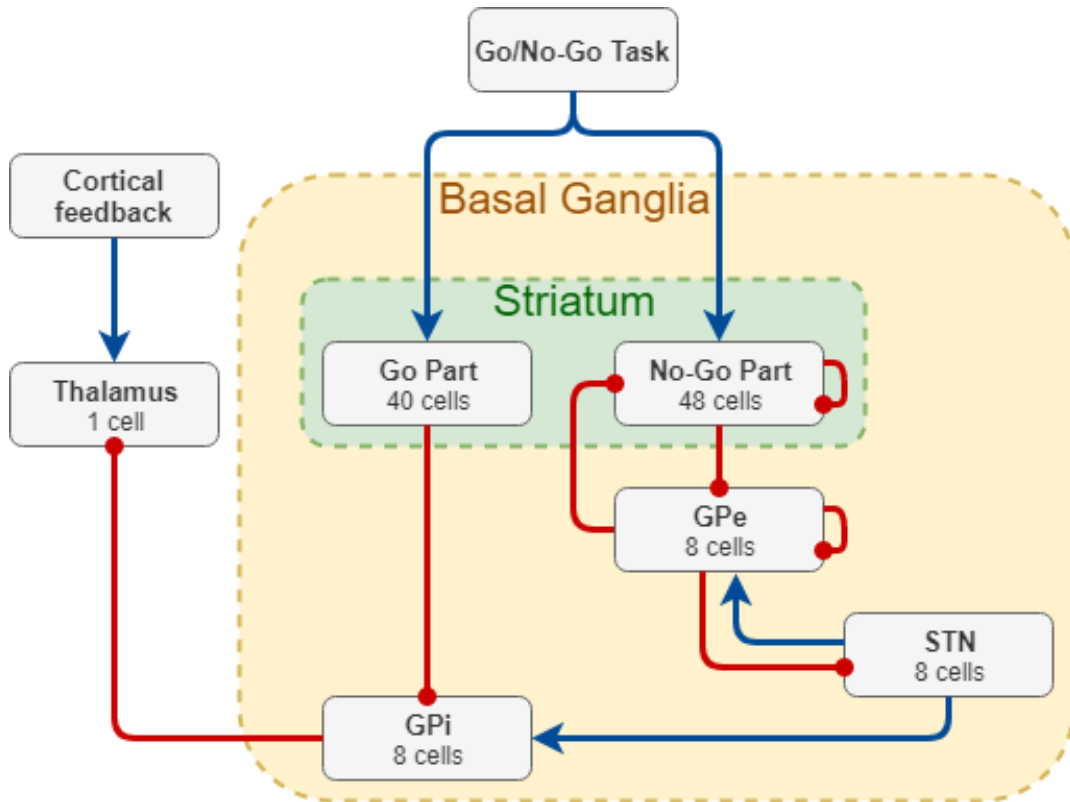

Figure 4. Scheme of the structure of the modeled network with the corresponding connections between the different regions of populations and the number of cells for each population. The blue lines indicate the excitatory connections and the red lines indicate the inhibitory connections.

$$H_\infty = \frac{1}{1 + e^{-\left((Vg_j - \theta_g) - \theta_g^H\right)/\sigma_g^H}} \tag{14}$$

where Vg_j is the potential of the presynaptic neuron j, θ_g is the is the half activation (or inactivation) potential of the corresponding neuron type, θ_g^H is the half activation voltage of the Heaviside step function and σ_g^H the slope factor.

Finally, the last current included in Eq. (1) was the I_{App} which refers to external currents that do not come from other populations of neurons. It was the case for the DBS, which is an external input applied to the STN and did not come from the network.

The different populations of neurons were implemented with their own characteristics, resulting in variations of some of the equations and currents included on each population. Besides, different connections were implemented for each population and number of cells were adjusted for the necessary connections. The structure included in this model is shown in Figure 4, as well as the number of neurons that conformed each population in the model.

i. Globus Pallidus

Beginning with the globus pallidus, both GPe and GPi were modelled in a similar way. As shown in the paper of *Rubin et al. 2004*, only some differences are present in those two populations as they are formed by the same type of neurons.[33] The most relevant differences in the implemented variables for these two populations were the synaptic currents as they have different inputs and outputs.

GPe received inhibition from the No-Go part of the striatum, inhibition from the other GPe cells and activation from STN cells. The first connection was made in a ratio 5:1, making a random structure (Figure 5B) of connections with the condition that five medium spiny neurons (MSNs) inhibit one GPe cell. The second connection was based in the principle of "winner-take-all", as neurons from the same population fight for their activation and when one is able to fire it inhibits the others. In this model, the neurons from GPe inhibited the two nearest neighbors, allowing other neurons from the same population to fire, but not those that are more proximal, known as "soft winner take-all" (Figure 5A). The activation coming from the STN was due to the loop formed by these two structures, in which each of the neurons of the STN activated one random GPe cell. Two conditions were imposed: all GPe cells should get at least one connection coming from the STN and the number of STN neurons was the same as the number of GPe neurons. It resulted in all the GPe neurons receiving one excitatory input from the STN.

With respect to the GPi population, the connections were similar to those shown in the GPe. The STN was also activating the GPi with the same structure that it did on the GPe and there was inhibition coming from the striatum. The difference was that the inhibition of the GPi came from the Go part of the striatum, but keeping the same ratio of connections and structure of the connections from the striatum to the GPe (Figure 5B).

ii. Subthalamic nucleus

To obtain a realistic model, a different approximation had to be applied to the low threshold Ca^{2+} current of the STN neurons. This modification was made to capture the difference of more prominent bursting in STN neurons caused by the effects of a

hyperpolarization-activated inward current to the T current.[27] This modification was seen in the corresponding T-type current:

$$I_\text{T} = g_\text{T} a_\infty^3 b_\infty^2 (V - E_\text{T}) \tag{15}$$

where b_∞ is the steady-state of the inactivation gating variable b, which captures the inward current besides the T-type current. This variable, instead of directly being a function of the voltage, it is a function of the gating variable r (which does depend on the voltage):

$$b_\infty = \frac{1}{1 + e^{(r-\theta_b)/\sigma_b}} - \frac{1}{1 + e^{-\theta_b/\sigma_b}} \tag{16}$$

where θ_b is the half inactivation potential of the variable b and σ_b is its slope factor.

With respect to the network inputs into the STN one input was added to the model. This input consisted in an inhibitory input from the GPe into the STN. This connection was arranged so each GPe inhibited three different STN neurons, which were the three nearest to each GPe (Figure 5A). The input from the cortex to the STN was not included in the model as it conforms the hyperdirect pathway which activity and relevance has been demonstrated, but its activity occurs before the activity of the indirect pathway, not affecting it but masking its activity in the subsequent β-band analysis as it was seen in the initial simulations where it was included, so it was finally kept out of the model.

iii. Striatum

Go part

The final compartment of the basal ganglia was the striatum. This compartment was modeled in two parts, the Go part and the No-Go part. The Go part of the striatum is the one that is part of the direct pathway, being part of the final activation of the thalamus. This compartment was modeled as it has been commented previously, with a ratio 5:1 with respect to the GPi, GPe or STN neurons in terms of number of neurons. The neurons modeled in the Go part were MSNs as more than 90% of this nuclei consists of MSNs,
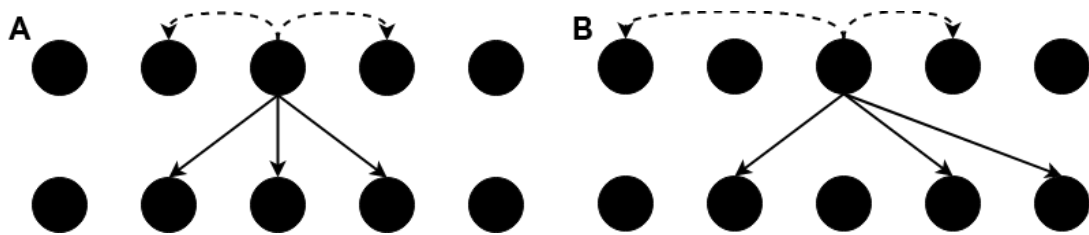

Figure 5. Different kind of connections used to communicate between populations of neurons. The upper row of each image represents the neurons of one population and the lower row represents neurons from a second population. Figure 5A is an example of the connections of one cell with the neighbors of the same population and the nearest neighbors of a second population in case that acts in two of the same population and three of the other population. Figure 5B is the example of random connections with the same and other populations, acting on the two in the same population and on three in the other population. In the modeled network, the number of cells that each population acts on does not have to be the same, but they can coincide with the ones of the picture, it is to give an idea of the differences between structured and random connections.

which had a slightly different approach to the ones of the globus pallidus and STN, not including the I_T and I_{AHP}.[32][36][37] I_T influence on the activity of MSNs is low enough to be negligible, so this current was not included in the model, reducing the necessary computational power to run the model. I_{AHP} was not included in these neurons as the recuperation from the I_{AHP} is slow and did not use the fast recuperation obtained with this current. Then, MSNs were modeled only with the following intrinsic currents: I_K, I_{Na} and I_{Ca}.

With respect to the connections, the only synaptic connection modeled for the neurons of the Go part were the inhibitory connection of MSNs to other MSNs. The connection implemented was the same as for the GPe, so every MSN was inhibiting his two nearer neighbors (Figure 5A). The input for the Go part was coming from the cortex, and then the input was modeled with an approximation of a sinusoidal signal explained later.

No-Go part

The other modeled part of the striatum was the No-Go part. This part of the striatum is the origin of the indirect pathway which tries to inhibit the parts of interest of the thalamus. Unlike the Go part of the striatum, the No-Go part was modeled of two types of neurons, the fast spiking interneurons (FSIs) and the MSNs, being a total number of neurons for each type of 8 and 40, respectively. The MSNs intrinsic currents were modeled the same way as in the No-Go part, but for the FSIs only the I_K and I_{Na} were used, as the neurons were expected to fire at very high frequencies in the order of 40Hz, with no bursting and a fast firing that did not need I_{AHP}. However, the number of FSIs was the same as in most of the compartments modeled, instead of the 5:1 ratio of the MSNs.[32][37]

The connections of this No-Go part were structured as an inhibitory loop with the GPe. Beginning with the FSIs, they received an inhibitory input from the GPe where each FSI was inhibited randomly by one GPe neuron (Figure 5B). Furthermore, every FSI inhibited his two nearest neighbors (Figure 5A). Inputs for the MSNs were similar to those of the Go part, but they received an inhibitory input from the FSI, which acted as intermediaries between the GPe neurons, each FSI inhibiting five MSNs with a random structure of connections (Figure 5B). These three populations built a small loop between the GPe and the No-Go part region of the striatum, known as the pallidostriatal loop. MSNs also received inhibition from their neighbors (Figure 5A) and an input from the cortex modeled similarly to that of the Go part.

iv. Thalamus

The final modeled compartment of the network was the thalamus. Only one neuron of the thalamus was done because it needed inhibition from 8 GPi cells each time, which would result in a high increase of the computational power needed as it would finally affect also the number of cells of the other populations. The neuron of the thalamus again contained the I_T, but not the I_{AHP}. For this compartment, the variables were reduced by one implementing a dependency I_K in function of h instead of n, reducing the computational power necessary for the system. Referring to the connections, the thalamus had two inputs, one coming from GPi and another simulating the input from the cortex. GPi was the common point for all pathways of the basal ganglia before reaching the
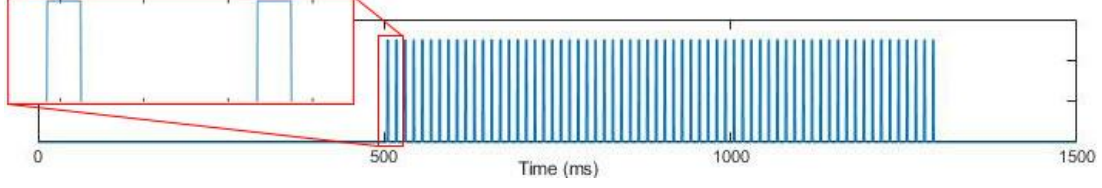
Figure 6. Model of the stimulus applied in the action selection tasks as a simulation of the input from the cortex to the striatum. Signal behavior was modeled similar to the behavior of spikes, which stay around 2ms depolarized, so this behavior was tried to be copied.

thalamus, where a connection with an inhibition ratio of 8:1 was implemented. It implied that eight GPi neurons acted on one thalamic neuron. The input from the cortex was a low frequency signal of 10Hz which was an approximation of a sinusoid. This approximation was made with a Heavisde step function, obtaining a pattern which is more similar to the neurons firing than just a sinusoidal signal:

$$I_{\text{Cortex}} = iH\left(\sin\left(\frac{2\pi t}{\rho}\right)\right) \times \left(1 - H\left(\sin\left(\frac{2\pi(t + \delta)}{\rho}\right)\right)\right) \qquad (17)$$

where i is the amplitude of the stimulation, H is the Heaviside step function, ρ is the period of stimulation and δ is the duration of each impulse. Due to the idea was to better assimilate the shape of neurons, the value of δ was set to 2ms by comparing the length of the action potentials of other populations of neurons, the ρ was set to 0.1s following the most optimal result obtained by *Terman et al.* 2002, and i was also set to a low value as the frequency, taking a value 10, so its influence on the thalamus with respect to the GPi did not mask the activity of the second one.[27]

This approximation was made because it was of interest to make the signal have only positive values and be equal to zero when the sinusoidal signal should be negative. The second part of Eq. (17) allowed to obtain a narrow step function, better assimilating the firing of neurons.

Parameters for the model were taken from several papers which previously worked on similar models and if necessary, they were tuned to get the expected response. For example, when too much inhibition from one population to another did not allow the second to fire the connectivity was modified, or when the contribution of a specific current was not visible their parameters were modified to add their contribution. Articles used to obtain the parameters were *Terman et al. 2002*, *Rubin et al. 2004*, *Scheler et al. 2014*, *Zitelli et al. 2016*, *Mahon et al. 2000*, *Du et al. 2017*, *Gruber et al. 2003*, *Biddell et al. 2013*, and *Damodaran et al. 2015*.[27][32][33][36][37][38][39][40][41] All values used for the simulations were included in Appendix.

v. Go/No-Go task

Go and No-Go signals were modeled as approximations of sinusoidal signals to simulate the firing of neurons. This approximation was made again by means of a Heaviside step function (which depended on a sinusoidal signal). The input signals looked again like in Eq. (17). Values set for the Go and No-Go tasks were picked by trying a range of values for the amplitude and frequency of the signal. The duration of the impulse was set to 2ms again like the one from the cortex as it was supposed to also simulate neurons firing from the cortex.

Go and No-Go signals were simulated with the same approximation as both come from the same brain regions, the prefrontal cortex (PFC) and the anterior cingulate cortex (ACC). The main difference of the signals is the region they act on, being stronger for Go tasks on the Go part of the striatum and on the No-Go part during the No-Go tasks. The signal was manipulated so the amplitude and frequency was adapted to every task performed.

Simulations had a time length of 1500ms, with the tasks performed during 800ms in total, between 500ms and 1300ms. These timings to perform the tasks were decided due to the experimental data shown in *Benis et al. 2014*, with respect to the response of the subjects in these action selection tasks.[25] The shape of the signal and the length in the whole simulation is shown in Figure 6.

B. Parkinsonian approximation

To obtain a parkinsonian behavior of the network, some of the parameters were changed. The origin of PD comes from the degeneration of dopaminergic neurons of the SNc which directly act on the striatum.[1][2] As the SNc was not added to the model and the output of it could not be added to the striatum parts, the striatum features were modified in the model to simulate the increase or decrease of activity that they suffer from the connection with the SNc.

As shown in Figure 1, SNc connects to the Go part of the striatum by activating it and inhibiting the No-Go part. Then, the loss of DA in PD results in lower activation of the Go part and lower inhibition of the No-Go, obtaining lower activity in the first and higher activity in the second. These differences were reproduced in the model by decreasing the conductivity of the Go part of the striatum, resulting in lower activity of the compartment and subsequently altering the activity of populations that are part of the direct pathway. For the No-Go part, its conductivity was increased resulting in higher activity of this population and later modifying the populations that are part of the indirect pathway.

To find proper values for the conductivity of these two populations in a parkinsonian state, a range of values were implemented to the conductivity of each population until finding some that reproduced the expected behavior of the network in the same population and the thalamus, which was the output of the network. The values of the conductivity were modified adding or subtracting a value of 0.1 to the value of the original conductivity, e.g., if the original conductivity were set to 0.3 and it had to increase, the range of values was increased so they took values of: 0.4, 0.5, 0.6, etc., until the optimal outcome was visible. An optimal outcome was decided to be achieved when the thalamus firing rate was reduced (Figure 1) around 10Hz, which was considered an important decay as it is higher than the firing rate of most populations firing rate in resting conditions.

Not only the striatum is affected by the loss of DA, but also the STN is affected as shown in previous studies from cortex connections.[42][43][44] This fact slightly reduces the activity of the STN (less influenced than via the indirect pathway), so the conductivity of this compartment was also decreased like in the Go part and the same approach as in the previous cases was followed.

In the model, mild and severe PD were studied to find out if significant differences were possible to be found in the different cases. To obtain this difference, severe PD was

stated first following the aforementioned procedure, as the answer of the network is more exaggerated and easier to be detected. This severe PD was seen as the degeneration around the 80-90% of the dopaminergic neurons as it is said in *Poewe et al. 2017*, which reaches these values of degeneration for PD patients which have had the disease over 10 years.[1] Once severe PD was stated, mild PD was seen as earlier stages of the disease when the symptoms are already visible which have a degeneration around 20-30%, so the values for mild PD on the changed conductivities were picked at 25% of the difference between the severe PD and healthy cases.

A final feature of the model was included for this approximation which was the DBS applied to the STN for treatment. It was modeled with a Heaviside step function for the impulse and applied to the model once the Parkinsonian state was simulated.

$$I_{\text{DBS}} = iH\left(\sin\left(\frac{2\pi t}{\rho}\right)\right) \times \left(1 - H\left(\sin\left(\frac{2\pi(t + \delta)}{\rho}\right)\right)\right) \tag{18}$$

where i is the amplitude of the stimulation, H is the Heaviside step function, ρ is the period of stimulation and δ is the duration of each impulse. For the simulation, high and low frequency DBS were analyzed to show the behavior of the network, as high frequency stimulation should relieve the symptoms and low frequency do not or even aggravate them. The values picked for these simulations were $i = 200$ for both cases, $\rho = 0.0067\text{s}$ for high frequency DBS and $\rho = 0.0333\text{s}$ for low frequency DBS, and $\delta = 0.6\text{ms}$ for both cases, what mimics the short current pulse. In the model, DBS was applied to half of the modeled neurons of the STN as the electrode implanted treatments might not have the same intensity on all STN's neurons.

C. Model analysis

Analysis of the model consisted in seeing the evolution of β-band frequency in the different simulations and later its response when DBS was applied. In this kind of analysis, local field potentials (LFP) are used to analyze the response of STN as shown in *Benis et al. 2014*.[25] The Hodgkin-Huxley model gives the potentials of single neurons, so an approximation of the LFP was necessary in the model to be able to analyze the activity of the β-band, and the experimental data available to compare the results work with LFP.

Different approximations of the LFP have been used in neuroscience, so it is not a unique technique to perform this approximation.[26][44][45] In this model, to approximate the LFP of the STN, the synaptic variable computed that represents the input that will go from the STN to the GPi was used. It consists of the sum of the synaptic variables of every neuron from the population to see how the overall activity has an effect in the GPi, which is the one that is calculated in Eq. (13).

This synaptic variable was later used to analyze the activity of the network in response to Go and No-Go tasks. The analysis consisted in studying the activity of the β-band (frequencies between 13Hz and 30Hz) to find out if there was a difference in the activity in normal and parkinsonian states along the whole length of the Go/No-Go task. To do so, Welch's method was used in the synaptic variables to obtain the spectral density

estimation, with a Hanning window of two times the samples inside 2ms (due to the different simulations, the number of samples was not constant in the whole study).

From the estimation, only the frequencies corresponding to the β-band were selected and the total amount of activity in this band was computed. The model was run 10 times for each scenario with different initial conditions for the membrane potential, gating variables, synaptic variables, and rebuild the random connections between populations, to obtain multiple examples to allow a statistical analysis. A number of 10 simulations was picked as it showed that irregular values way above or below the mean, in a single simulation did not have a large influence on the final mean. In the parkinsonian state, the model was run three times for the initial conditions: without DBS, with low frequency DBS and with high frequency DBS applied to the STN to see if the effect of DBS in the model worked as expected, depending on if the DBS is of high or low frequency.

The statistical comparisons made were: healthy vs parkinsonian simulations, parkinsonian without DBS vs parkinsonian with high frequency DBS simulations, and parkinsonian without DBS vs parkinsonian with low frequency DBS simulations. The comparison of the values for the different simulations was performed by means of a 2-tailed student's t-Test when the populations' distribution was normal and a 2-tailed Mann–Whitney U test in those that were not normal to find if there was any significant difference between them.

To visually examine the results and see if it is valid to state that the response was caused by the action selection task, spectrograms were finally performed on the cases that showed significant differences. The spectrogram was used to see if the increase or decrease of the power observed in the analysis was inside the time length in which the action selection task, or the increase of β-band is mainly due to the parkinsonian state and is also visible outside the timing of the task.

3. Results

The main goal of the thesis was to build a computational model of the basal ganglia able to reproduce the effects of PD during Go and No-Go tasks and evaluate if the β-band of the STN can be used as biomarker of DBS.

A. Model validation

The model of the neurons is made following the Hodgkin-Huxley description of ion channels dynamics, obtaining the firing of the single neurons. Figure 7 shows the firing pattern of all the modeled populations of neurons which are part of the basal ganglia and the thalamus in a healthy state. It is seen in this Figure 7 that neurons are able to fire regularly without any external stimuli, but external stimuli are able to change the firing
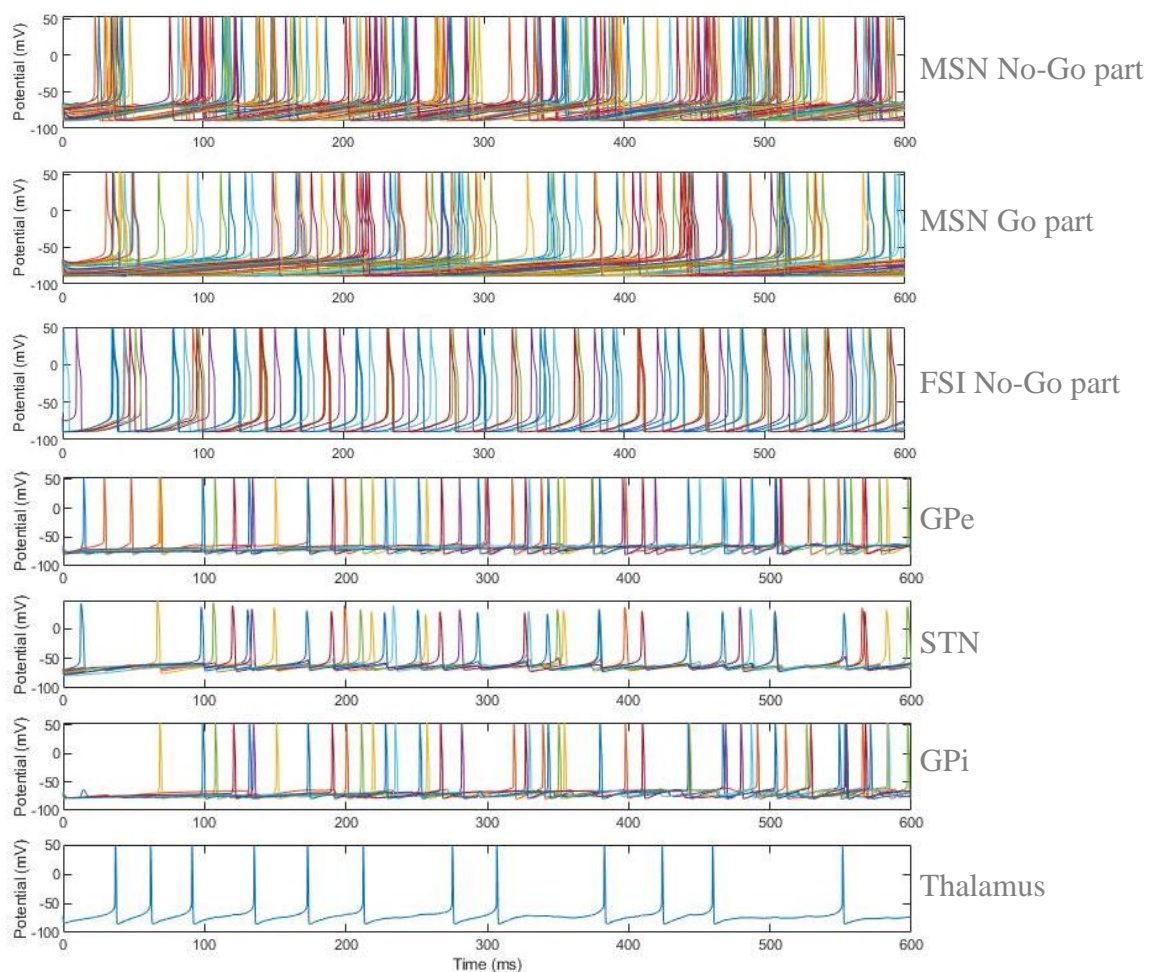

Figure 7. General response of the model when no external input is added to the network on a healthy simulation. From top to bottom, the graphs show the firing pattern of: MSNs of the No-Go part of the striatum, MSNs of the Go part of the striatum, FSIs of the No-Go part of the striatum, GPe neurons, STN neurons, GPi neurons, and thalamic neurons. Times for plots are reduced to 600ms to be able to have a clearer look on the graphs and are centered at times when the tasks are performed. It is the representation of the resting state, which would correspond to the time between 0 and 500ms of Figure 6. Each color is the representation of a different neuron, but for the Go part and the No-Go part the colors are repeated as there are 40 neurons on each case.
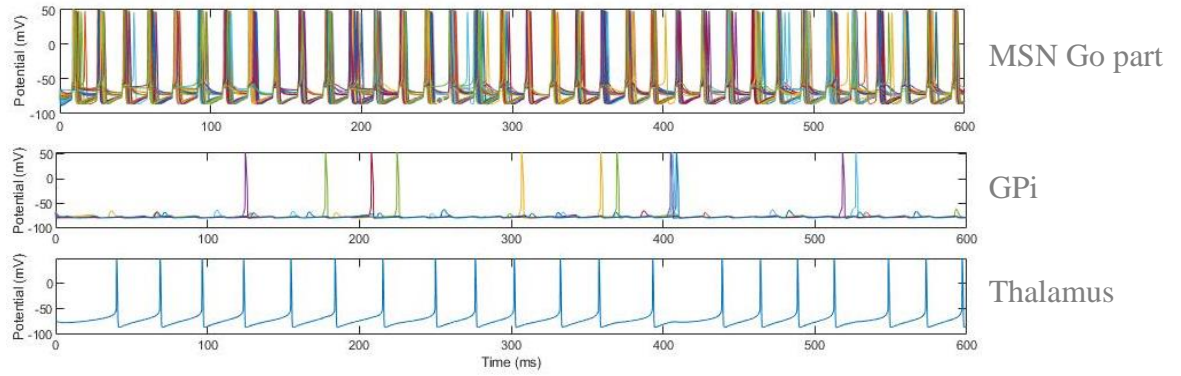
Figure 8. Response of a healthy simulation when a Go task is included in the model. The top graphs represent the firing pattern of the Go-part of the striatum, the middle one the response of the GPi, and the bottom the response of the thalamus. The Go-part becomes highly active, then GPi is inhibited with respect to the resting state, what leads to the disinhibition of the thalamus, which one becomes more active. The simulation is limited to the time of a Go-task is produced to show more clearly the neuronal response and 0ms would correspond to 500ms of Figure 6.

pattern as shown in Figure 8 and Figure 9. This initial simulation was used to evaluate the network and ensure that the response of the populations was according to experimental data and already proven models. For this evaluation, firing rates and patterns were evaluated from the different plots, calculating the mean firing of each population of

Figure 9. Response of a healthy simulation when the No-Go task is included in the model. From top to the bottom, the graphs represent the firing pattern of MSNs of the No-Go part of the striatum, GPe neurons, STN neurons, GPi neurons, and thalamic neurons. The activity of the GPe is mostly due to the activation of the STN, as it is inhibited due to the high activity of the No-Go part. The original inhibition causes the high activity of the STN, which acts on the GPi and finally increases its inhibition to the thalamus. Again, time limit is done like in Figure 8.

19

Figure 10. Response of a parkinsonian simulation when the Go task is included in the model. The top graph represents the firing pattern of the GPi and the bottom the firing pattern of the thalamus. The Go part of the striatum is not included as the compartments that show the most information about the final behavior of the model are the two shown. The activity of the GPi is increased with respect to the one in Figure 8 as the Go-part is not able to inhibit it, allowing a higher inhibition of the thalamus instead of its disinhibition as it should happen in Go tasks.

neurons and visually inspecting if the firing pattern corresponds to the one observed in papers.

Beginning with the initial population shown in Figure 7, to check the viability of MSNs of the No-Go part the model developed by *Corbit et al. 2016* was used as it already explained the behavior of a normal network without any external stimulus, together with the experimental data collected by *Lee et al. 2016*. It is shown that MSNs of the No-Go part fire at a frequency smaller than 10Hz, around 6Hz, which assimilate to the frequency obtained in the model of this thesis as it can be seen in Figure 7, as in 600ms each neuron fires between 3 and 4 times, obtaining a mean firing rate of 5.69Hz±0.57. FSIs, which are part of the same loop and described also in the same paper, should have a firing frequency between 20 and 30 Hz, which is also accomplished in this model as each neuron fires between 2 and 3 times per each 100ms, obtaining a mean firing frequency of 25.79Hz±3.11.[32][47] For the MSNs of the Go-part of the striatum, the frequency of firing was not stated in the *Corbit et al. 2016* but there is experimental data of the firing rate of MSNs in *Lee et al. 2016*. This paper shows that the firing frequency is slightly lower than
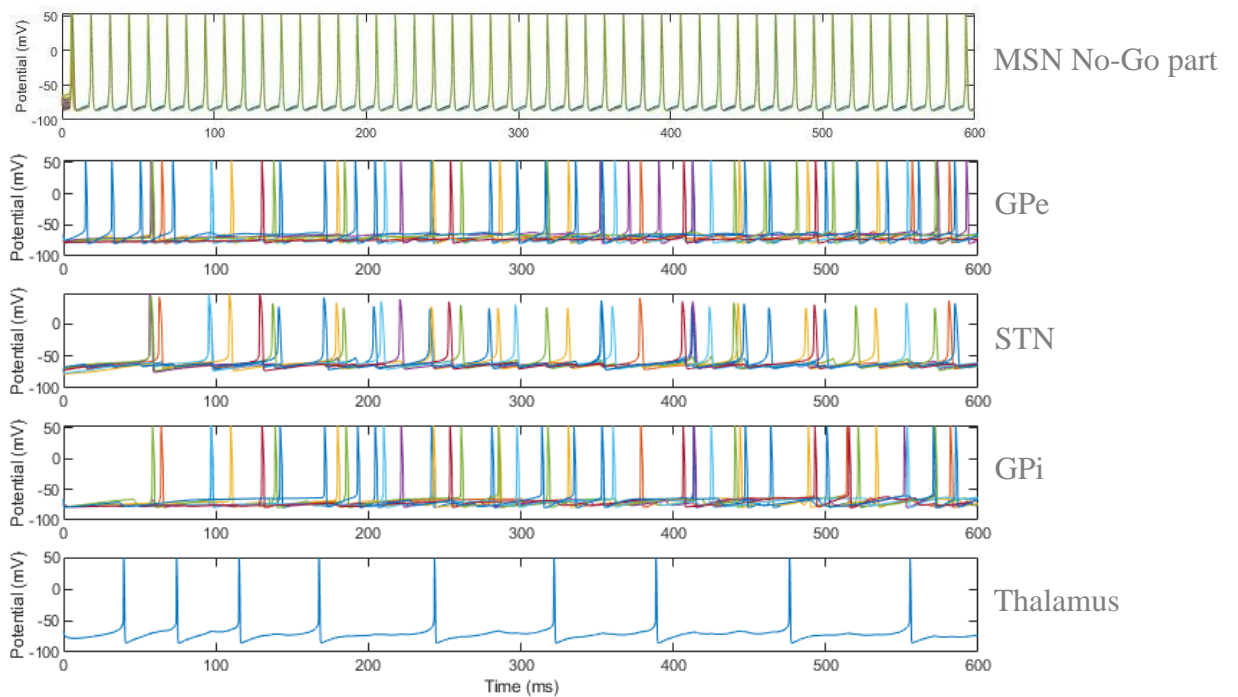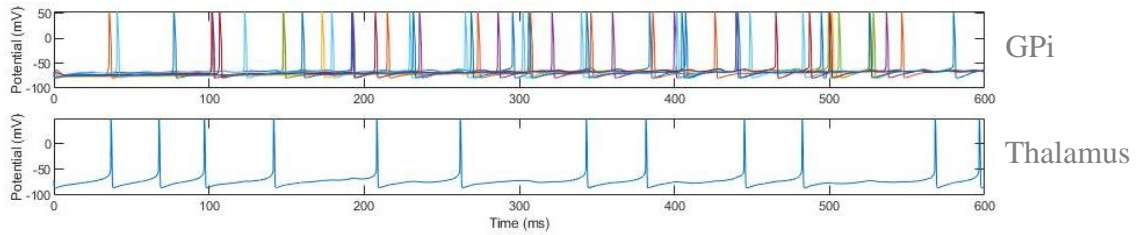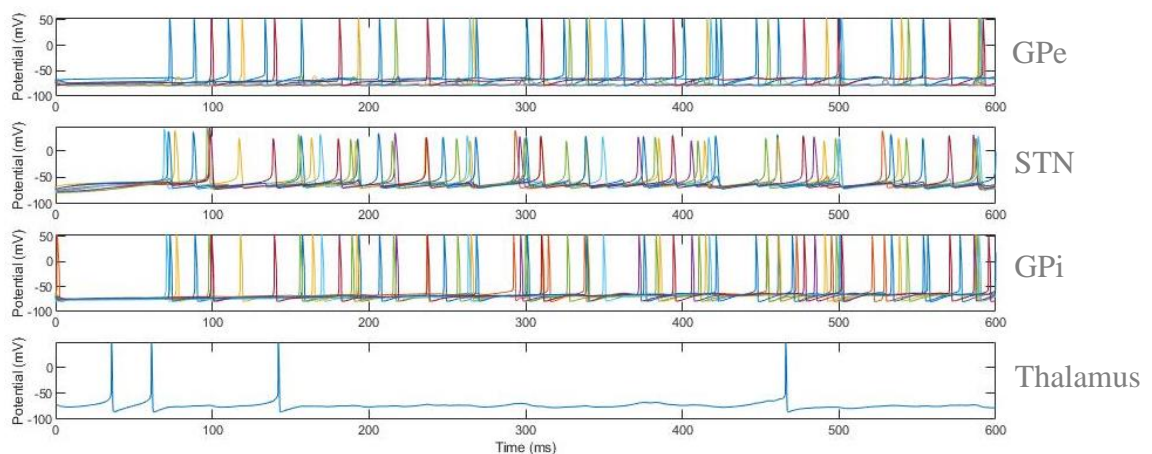

Figure 11. Response of a parkinsonian simulation when the No-Go task is included in the model. From top to the bottom, the graphs represent the firing pattern of GPe neurons, STN neurons, GPi neurons, and thalamic neurons. The No-Go part of the striatum is not included for same reason explained in Figure 10 for the Go-part. The GPe becomes more inhibited than in healthy cases like Figure 9.

in the No-Go part, near 4Hz. In Figure 7, the number of times the neurons fire during the 600ms is between 2 and 3, being more common the first one, obtaining also a realistic network as the firing frequency is 4.48Hz±0.75.[47] It might not be clearly visible in the figure, but individual inspection was made to ensure the realistic firing was satisfied in all populations. In all cases, firing patterns are similar to those of *Corbit et al. 2016*, with the MSNs trying to fire in between successful action potentials but getting inhibition from other cells, while FSIs fire at high frequency, recovering from previous repolarizations to rapidly fire again.[32]

With respect to the remaining GPe, STN, GPi and thalamus, they were mainly modeled from *Terman et al. 2002* and *Rubin et al. 2004*. Parameters chosen for the model were those that in the article were described as irregular or weakly clustered firing, to avoid obtaining the synchronization of neurons in the healthy simulation, as it would be considered more common in parkinsonian simulations. *Terman et al. 2002* obtains frequencies around 4-6 Hz, which was slightly increased in the model purposed to 8-10Hz because the activity of the thalamus did not receive enough influence from the previous populations of neurons, so parameters of the network were tuned to obtain a slightly different output.[27] The mean firing frequency for the GPe was 9.14Hz±0.76 and for the STN was 8.87Hz±0.83. Besides, in *Rubin et al. 2004*, neurons fire also at lower frequencies than the one expected in the model, so tuning was also applied in GPi and thalamus, obtaining mean firing rates of 8.57Hz±0.73 for the GPi and 20.81Hz±1.13 for the thalamus. However, firing pattern of the neurons in the model were similar to the originals but with higher frequencies, obtaining what can be considered a realistic behavior.[33] Bursting did not appear in the model as inhibition from the other connections avoided the neurons from repeatedly firing.

B. Model sensitivity

Modification of several parameters of the networks was also performed to see how erratic it behaves with little variations around 10% of its usual value, trying to find for which parameters the model is most sensitive. Biggest differences are found in resting potentials of the different ions, half activation voltages and slope factors. For three different kinds of parameters the network becomes highly erratic and in most cases the network is unable to fire, especially in the resting potentials.

Changes in slope factor what mainly differs from the final network is the duration of the action potentials, which need more or less time to complete the depolarization depending if its value was increased or decreased. However, in some cases like variations of the slope factor of the gating variable of K^+ and both gating variables of Na^+, the network became unable to fire, even for small changes. With respect to voltage dependent parameters (resting potential and half activation voltage), the network is the most sensible to changes and this small changes of 10% cause important errors in the network, which becomes unable to fire, getting a flat line as a result of the neurons action potentials.

Other parameters like conductivity and activation time constants variations do not have a large influence with respect to their standard values. The 10% change in values in these parameters mainly resulted in changes in the firing rate. The conductivities make them more likely or not to have an influence in the action potential, so neurons become more
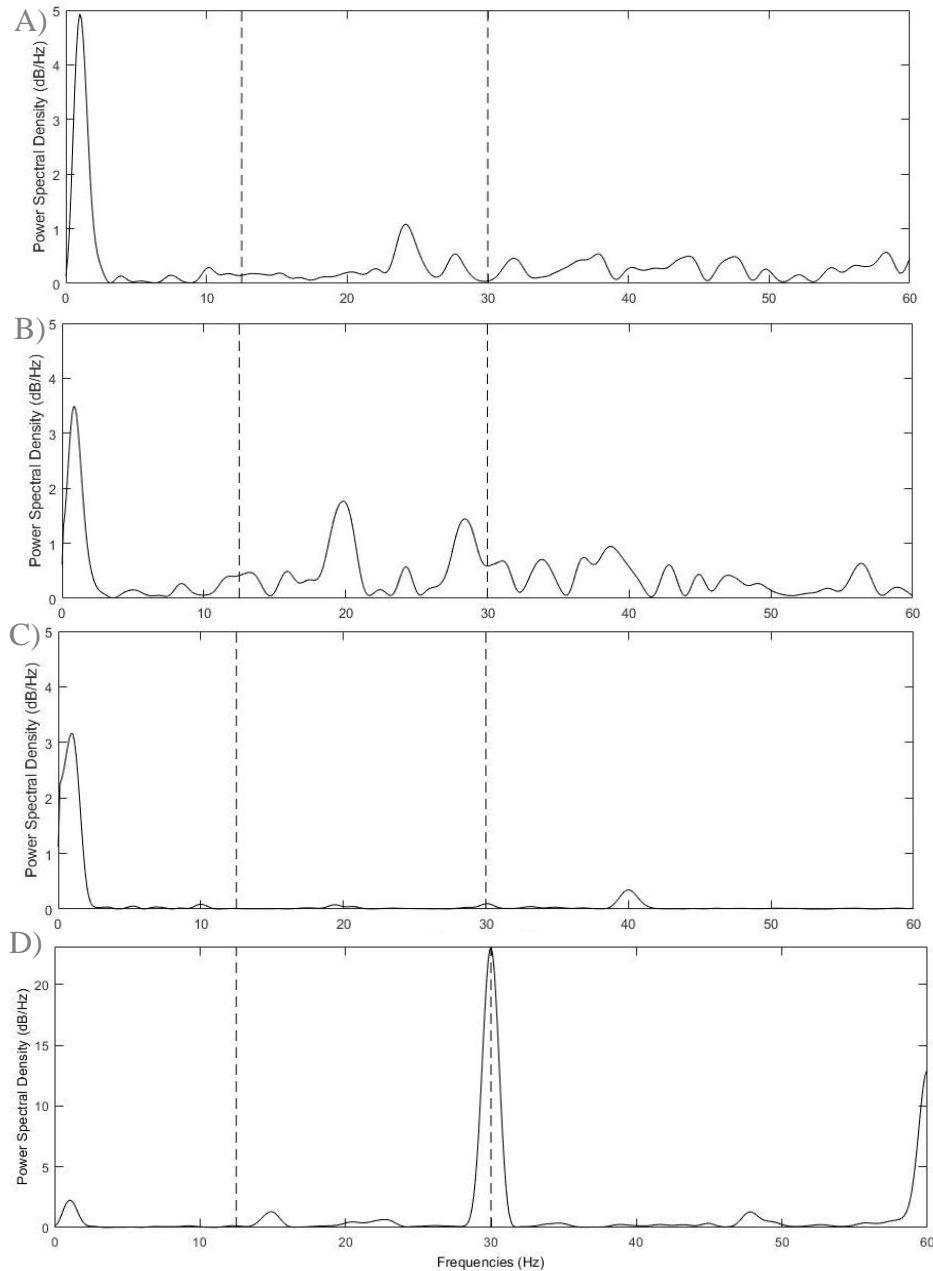
Figure 12. Power spectral density plots of the different simulations run. A) PSD of the healthy simulation, B) PSD of a severe parkinsonian simulation during a No-Go task, C) PSD of the high frequency DBS, and D) PSD of the low frequency DBS. Limits of the β-band are indicated by the dashed lines and it is visible how the density on the parkinsonian plot increases with respect to the healthy simulations. Furthermore, when looking at the β-band in high frequency DBS, these frequencies almost disappear, while in in low frequency DBS significantly increases.

excitable when conductivities are increased. Activation time constants also affect excitability, but they work inversely. Neurons become more excitable with lower time constants as less time is needed to be active after firing previously.

C. Action selection tasks and parkinsonian simulations

The goal of the model was to see its response when action selection tasks are applied and this is what happens in Figure 8, when a Go task is included in the model. A Go task stimulates mostly the Go part of the striatum. Figure 8 shows this behavior by increasing

the firing frequency of this population and due to their connections, it inhibits the GPi, which activity is seen reduced and the GPi finally cannot inhibit the thalamus, which becomes more active.

The response when a No-Go task is executed appears in Figure 9. This kind of task activates mostly the other part of the striatum, causing a cascade of activations and inhibitions of the populations of neurons of the indirect pathway, beginning with a higher activity of the No-Go part of the striatum and finally partially inhibits the thalamus as seen in Figure 9. Activity is slightly decreased with respect to the non-stimulated simulation as more activity of the No-Go part of the striatum leads to higher inhibition of the GPe, which cannot inhibit the STN (only when the same STN activates the GPe and it avoids the same neuron from the STN to fire rapidly again) and this increases the activity of the GPi, which finally inhibit more the thalamus, avoiding its activation. Comparison of the thalamus activity in Figure 7 and Figure 9 shows how in the first one, the thalamus is able to fire 12 times while in the second 9, in the same length of time.

When PD conditions were added to the model, certain differences appeared in the behavior of the system, being them visible in the firing patterns of the different populations of the network. For the Go-task, it has been already mentioned that the activity of the Go part of the striatum is decreased due to the loss of DA from the SNc, what leads to lower inhibition of the subsequent population of neurons which is the GPi (Figure 1). It is shown in Figure 10, when compared with the previous GPi firing pattern when a Go task is performed in healthy subjects, that the activity of this population is increased. This leads to the decrease of activity of the thalamus as it receives more inhibition from the GPi.

On the other hand, the No-Go task mainly affects the indirect pathway and the loss of DA characteristic of PD leads to higher activation of the No-Go part of the striatum, what turns into higher inhibition of GPe. It is seen in Figure 11 how the GPe fires less than in healthy cases and it is mainly able to fire when the STN activates it. Colors of the GPe and STN in the figures are shared for those of one population that correspond to the same of the other. GPe neurons are most of times activated few ms later than the same of the STN, showing the commented activation due to the connection between these populations from the STN to the GPe. The STN is also more active due to the reduced activity of the GPe, activating the GPi and finally inhibiting the thalamus. The final inhibition of the thalamus is higher than in the healthy case, becoming a possible reason of the problems that PD patients show when they try to perform a No-Go task.

D. β-band and DBS analysis

The model was designed to find the differences in activity of STN's β-band in healthy and PD simulations, and finally see if DBS changes this frequency, so STN's β-band could be used as biomarker. The results of differences of β-band power were made with populations of 10 simulations per each case (healthy Go, healthy No-Go, parkinsonian Go, parkinsonian No-Go, parkinsonian Go with DBS, and parkinsonian No-Go with DBS). This repetition of each case was made to obtain more than one case and be able to perform a more trustful study. Figure 12 shows the power spectral density (PSD) of the

different simulations during a No-Go task and it gives an initial idea of how the β-band actually increases in parkinsonian simulations with respect to the healthy ones.

Results showed that significant differences in the β-band were not possible to be found between healthy and mild parkinsonian simulations when performing a Go task (two-tailed Student's *t*-test gave a *p*-value=0.976). As shown in Figure 13, differences between healthy and mild parkinsonian have very similar values, so it is expectable not to find significant differences. When No-Go tasks were performed, significant differences in the β-band neither were possible to be found between healthy and mild parkinsonian (*p*-value=0.085). The difference with respect to the Go task is that the *p*-value is almost in the limit, and in Figure 13 is visible how a little increase in the power of the β-band is appreciable.

When the conditions of PD were set as severe, the analysis showed that significant differences in the β-band were not possible to be found between healthy and severe parkinsonian cases when performing a Go task (*p*-value=0.6). Like in the case of mild, Figure 13 shows how the differences in power were minimum and differences were not possible to be found. On the other hand, when a No-Go task was performed the same test gave significant differences in the β-band between healthy and severe parkinsonian cases (*p*-value=0.0). These differences are visually presented in Figure 13, where the mean with its standard deviation are shown .

When comparing if mild and severe parkinsonian states had significant differences, results showed that in Go tasks significant differences in the β-band were not possible to be found between mild and severe parkinsonian cases (*p*-value=0.557). Again, the differences are almost inappreciable and this was reflected in the result of the test. However, when the simulations were of a No-Go task the increase is again visible and this time significant differences in the β-band were possible to be found between mild and severe parkinsonian cases (*p*-value=0.04).
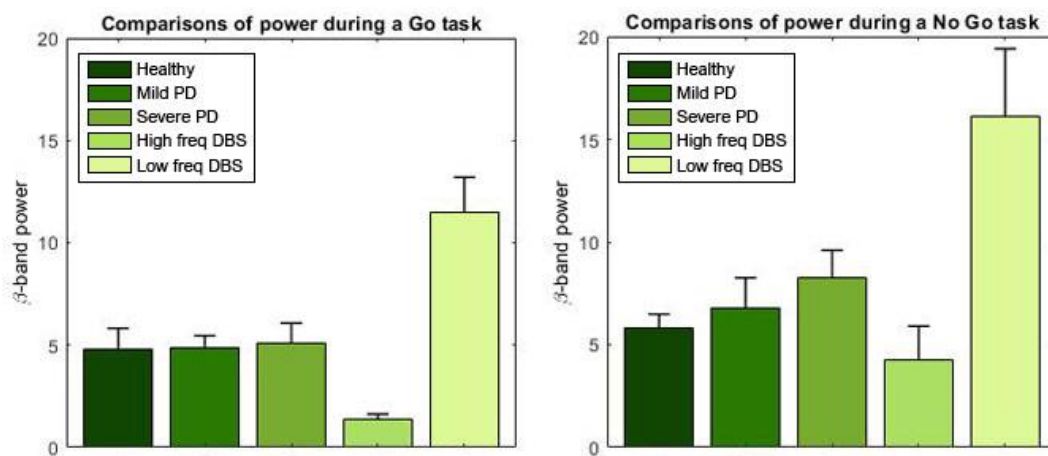
Figure 13. Bar graphs of STN's β-band power of the different simulated cases for the Go task (left graph) and No-Go task (right graph. It is noticeable the continuous increase of β-band power in the No-Go task as PD aggravates and the drop of the β-band power in high frequency DBS cases for both tasks, while for low frequency DBS the β-band increases a lot. For the Go task, the difference in β-band is less significant as PD aggravates and the same response the network has for the No-Go task also when DBS is applied.

In addition, the response of STN's β-band when this same region received high frequency DBS for parkinsonian patients showed that the differences in both tasks were significant (*p*-value=0.0, for both cases). Figure 13 includes the response of the β-band when DBS is applied on the right bar of both graphs, showing a decrease of the power as expected. When the low frequency DBS stimulation was also applied, the increase of β-band showed that the differences in both tasks were significant (*p*-value=0.0, also for both cases). A huge increase in the β-band was visible, having values over 10dB/Hz in both cases, doubling the values of severe conditions.

Evaluation over time was also visually inspected by means of the spectrogram which is seen in Figure 14, where the comparison of a No-Go task is made between a healthy and severe PD simulation. The second case showed higher power in the frequencies of the β-band (around 20Hz specially) within the time in which the No-Go task was performed, which in both cases was from 500ms to 1300ms. Furthermore, when looking at the frequencies before the task is performed, it is visible how the activity in the β-band was significantly smaller, but some can still be observed.
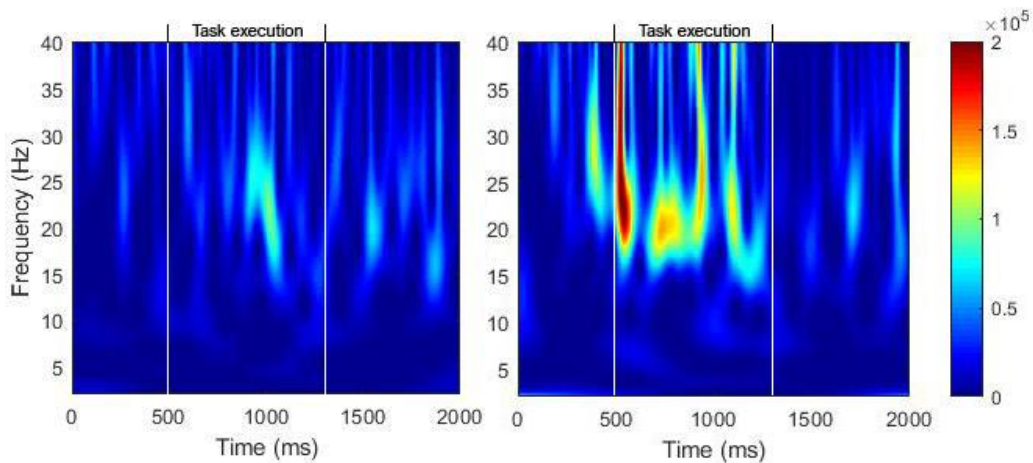

Figure 14. Spectrograms of the modeled during a No-Go task performed between 500ms until 1300ms. The spectrogram of the left is a healthy simulation and the spectrogram of the right is a severe PD simulation. It is visible how the frequency in the β-band is enhanced in the parkinsonian simulation, as seen in the previous Figure 13.

4. Discussion

The main goals of the thesis were: 1) design a model of the basal ganglia able to reproduce PD symptoms in the different neural populations that take part in the cortico-basal ganglia-thalamocortical during action selection tasks (Go and No-G tasks), and 2) study if β-band can be used as biomarker for DBS on PD cases.

The designed model was initially a version of the model developed by *Wiecki et al. 2013*, where a model for inhibitory control of the cortico-basal ganglia-thalamocortical loop is done.[48] In this paper, the model consisted of multiple neurons grouped together into layers to obtain a system level model where the mean firing rate in a period was used to calculate the level of activation of each group, taking into account inhibitory, excitatory and leakage currents as one group each one. On the other hand, in the model presented in this thesis the firing of single neurons along time was calculated and they were not grouped to compute just the activation of a certain group, taking also into account the properties of the individual contribution of different ions to produce the action potentials. The main idea to use the purposed model by *Wiecki et al. 2013* was due to the relevance of the striatum they show in the paper when action selection processes take part, like in Go/No-Go tasks.[48]

If the response of the network is observed in healthy simulations, both Go and No-Go tasks show the expected responses. In the first case, Go tasks are those that require the movement of subjects to be performed, what implies that certain signals must be sent from the cortex and higher activation of this zone is necessary. This higher activation of the thalamus is acquired by means of its disinhibition, as the GPi gets less active and cannot send the inhibitory signals to the thalamus. It is shown in papers like *Wiecki et al. 2013* or *Frank 2006* the main role of the thalamus for the activation of the cortex in motor tasks, so the higher activity obtained in the thalamic neurons during the Go tasks becomes a proper outcome for the network.[48][49]

In the case of the No-Go tasks, movement has to be avoided, what would cause to have less activation of the thalamus and cortex with respect to the Go tasks. The model is able to reproduce this behavior as the firing frequency of the thalamus is reduced, but not completely eliminated. It makes sense as a complete inhibition of the thalamus signal would not allow the activation of the motor cortex at all, and then would not allow a minimum voluntary motor control. This kind of response is again seen in *Wiecki et al. 2013*, where the activation of the thalamic cells in inhibitory tasks is reduced with respect to Go tasks but certain activity is still present in these populations of neurons.[48]

If moving to parkinsonian simulations, alterations on the behavior of such population is seen and they became actually visible also in the developed model. The common output in PD was already shown in Figure 1, where the thalamic activity is reduced as the inhibition coming from GPi is generally increased because of receiving higher activation or smaller inhibition. This is supported in several papers which show that the cortical activity is reduced in PD, which activity is influenced by the activity of the thalamus that also decays.[50][51][52]

In the Go tasks for the model, the activity of the thalamus is reduced with respect to the healthy simulations due to the higher activity of the GPi. This higher activity of the

GPi was possible due to the loss of DA in the SNc, which activates the Go-part of the striatum. The loss of DA in the model was introduced in the model by reducing the conductivity of the neurons of the Go-part of the striatum what resulted in the disinhibition of the GPi with respect to the healthy cases, as the first population was unable to inhibit the second one.

No-Go tasks also showed the decay of activity in the thalamus, having a similar behavior to the Go tasks but more exaggerated, as the decay of the frequency is larger. This could be an explanation for the problems that PD patients tend to show on inhibitory control, which is seen in *Benis et al. 2014*, where patients are unable to successfully perform the inhibitory actions.[25] The huge decrease of the activity in the thalamus could be an explanation for the freezing episodes seen in these kind of tasks of PD patient, causing the unsuccessful inhibition. Also, this could be an explanation of why the reaction times in inhibitory tasks have also larger delays in PD than Go tasks in some papers, as maybe the larger decrease of activity could increase the difficulty of performing the tasks.[22][25]

With respect to the study of the β-band in the STN and the application of DBS, the results obtained in the model could be an indication that β-band power could be used as biomarker for the application in PD patients, meaning that DBS is switched on when β-band is above certain threshold. Results of the β-band showed an increase of the β-band power for No-Go tasks in severe PD simulations with respect to healthy, which partially coincide with the findings of *Kuhn et al. 2004*.[18] In this article, the β-band power increased in No-Go tasks for severe PD subjects as shown in this model, but the Go task took the opposite effect and decreased, while in this model it kept a similar value as in healthy simulations, not having significant differences according to the performed tests. This could be due to the lower participation of the STN in the Go task, and as the model does not contain the cortex or the hyperdirect pathway, its activity might not be influenced as much as in the mentioned paper, obtaining this different result.

For mild PD, differences in the β-band were not significant in any task. For the Go task the difference was minimum, while for the No-Go task it increased (but not significantly) coinciding again with *Kuhn et al. 2004* in the second case but not in the magnitude of the difference.[18] What might indicate the results is that the increase of β-band within the progress of PD is caused by the decrease of inhibition of the STN by the GPe, showing that the β-band oscillations are due to the lack of inhibition of the STN. This could imply that the normal state of STN without the physiological connections of healthy cases oscillates at the typical frequency of PD, and as less connections it has due to the progress of PD, it becomes abler to oscillate at the β-band frequency.

When looking at the β-band power when high frequency DBS is applied, the results showed the expected decrease of β-band that appears when PD patients receive this treatment as explained in *Brown 2007*, as high frequency DBS is supposed to suppress these oscillations.[19] In the model these oscillations were significantly reduced, obtaining a mean value below the healthy conditions but some activity at the frequency band is still present (which would be necessary to perform the tasks), and in both Go and No-Go tasks significant differences were possible to be found between with and without DBS simulations. The difference between healthy and high frequency DBS might be caused

by the limitations of the model, and a complete model maybe could result in very similar values. On the other hand, low frequency DBS has the opposite effect, enhancing the β-band power and being a possible explanation of why low frequency is not only ineffective to deal with PD, but it can aggravate the symptoms, as the β-band oscillations are more prominent than in parkinsonian simulations. With these results, it seems feasible to use β-band power in the STN to know if DBS application is working properly as the simulation showed a clear decrease or increase on its power when applied.

However, the decrease of β-band present in high frequency DBS might also become a problem for task execution as some β-band is necessary for inhibition tasks as shown in healthy simulation of Figure 13 and several papers.[18][22][25][30] Subjects might become unable to perform the No-Go task correctly as the thalamus could not be activated enough due to the high activity of the STN, which finally causes the inhibition of the thalamus. Besides, the application of DBS can cause impulsivity as stated in *Frank et al. 2007*, where the subjects show problems to withhold their response in conflict situations like action selection tasks.[17] The results obtained in this model could indicate that the visible decrease of β-band when high frequency DBS is used might be a reason for this impulsivity, and then imply that higher levels of β-band might be still necessary to avoid this impulsivity, as some activity in this frequency band is still visible in healthy cases.

Response of the spectrograms showed a similar response to that of *Benis et al. 2014*, where the change of the β-band for stop tasks in healthy cases was more discrete than in parkinsonian cases with respect to the previous time.[25] Moreover, the response in healthy cases is more visible a few milliseconds after the start of the No-Go task, while in the parkinsonian cases the increase of the β-band is more abrupt and this increase is more sustained in time than in the healthy cases like shown in Figure 14, indicating that the approximation of the action selection task is appropriate.

These results could be used to answer the initial question to see if β-band could be used as biomarker for treatment of patients with DBS. When high frequency DBS is used the model showed that the power of the β-band should diminish to values slightly lower than in healthy conditions and for low frequency application the increase should be large. Then, β-band at the STN during the application could be considered a good option for such task.

The model could be considered a good approximation of the physiology of the cortico-basal ganglia-thalamocortical loop as the firing patterns and rates of the populations of the network were the expected, and then it exhibited the relevance of the striatum for action selection tasks, modulating the activity of the thalamus depending on which part of the striatum is activated. This outcome might lead to examination of other processes to see if the results would also coincide with experimental data and prove that the model could be used to completely describe the role of the different parts of the loop. Nevertheless, before exploration of other processes the limitations of the model that are commented later should be fixed to make sure that the effect that they might have in the model is taken into account.

Regarding PD, this model also displayed the importance of the striatum in PD and why PD patients tend to show more difficulties in executing No-Go tasks than Go tasks. In both cases the activity of the thalamus was overinhibited and in both cases the changes

were mainly produced in the striatum to simulate the degeneration of DA paths from the SNc. The inhibited thalamus seems a reasonable explanation for the key role that has the striatum in the malfunction of PD subjects, as the thalamus is the region connected back to the cortex and its inhibition may lead to motor and cognitive problems. With respect to the difficulties shown in the tasks, the differences of the β-band in the STN for No-Go tasks seem a proper explanation to recognize one source of malfunction in PD. No-Go tasks are usually worse executed in parkinsonian cases and they are the tasks that showed alterations in the β-band, while Go tasks barely did. Then, the model showed how the degeneration of DA pathways to the striatum are the source of PD and how the cascade that follows the striatum alter the activity of the patients, causing significant differences in the STN for the most problematic tasks.

The application of DBS showed why its effects can be beneficial for PD patients as it reduced the increase of β-band they suffer. However, it also showed some differences with respect to healthy subjects which might be the explanation for the problems of impulsivity that appear in some cases when DBS is applied. As the behavior of the model could be considered optimal, this model could then be used to see if stimulation of other regions of the brain could also lead to most optimal results, not only decreasing the activity of the β-band, but also obtaining values more similar to the ones obtained in healthy simulations.

Model limitations and future work

Despite the results obtained in the model looked promising and similar as what was expected, some more features should be included in the model as they could not be included and their inclusion might change some of the results, as it is known that they take a role in the cortico-basal ganglia-thalamocortical loop.

One of the main differences between the presented model and the one from *Wiecki et al. 2013* is the inclusion of the cortex. It is clear that cortex may take an important role in the action selection process and the feedback it gives to the basal ganglia after the stimuli is processed until the thalamus as it closes the loop, but several parts of the cortex would have to be modeled and they were not possible due to lack of experimental data and lack of models of the necessary neurons.[48]

The ACC is known to have a role in the process of action selection but it was not possible to be modeled as it is mostly composed of spindle cells, which data was not possible to be found. So to model them, corresponding experimentation would be necessary to be able to model this region. Moreover, frontal eye fields (FEF), dorsolateral prefrontal cortex (DLPFC), supplementary eye fields (SEF), and pre-sensorimotor area (pre-SMA) are known to also have a role in the process, but specific parameters about their populations of neurons were neither possible to be found, due to lack of time and the high amount of compartments that had to be modeled, and all regions' pathways are supposed to go through the ACC in this kind of activities, so their signals would not be able to be integrated to the network. It caused that the cortex was introduced in the model as approximations by means of input-output functions, which do not completely copy the behavior of this brain region.

Another limitation of the model was the non-inclusion of the SNc. This region is known to be one of the origins of PD due to the deterioration of its dopaminergic neurons and their connection with the striatum might have large importance in action selection tasks. In the model their effect in populations are already included in the healthy simulations and its deterioration is seen as modifications in the conductivities of the affected populations because of the lack of the original signal, so their modeling is not fully accurate.

5. Conclusions

In this thesis, a model of the cortico-basal ganglia-thalamocortical loop was successfully developed to test its response in PD. The behavior of the model in healthy resting state was compared with experimental data and previously developed models to validate the network and ensure a realistic response. The lack of the model was that it could not include all the compartments of the loop, and their activity had to be compensated with input/output functions simulating their signals to other parts of the neurons.

With respect to the action selection tasks, they were successfully modeled to the striatum to show their importance in the loop for this kind of tasks. The activation of the direct pathway caused the activation of the thalamus due to its disinhibition, which is expected for Go tasks, and the activation of the indirect pathway increased the inhibition of the thalamus, which is expected in No-Go tasks to avoid the movement. Furthermore, when the conditions of the network were adapted to those that should appear in a parkinsonian state (both mild and severe), the outcome was the expected, showing the increase of the β-band that has been observed in previous experimental studies as PD progresses, and how the activity of the thalamus decreased in both cases, being a probable reason for the freezing episodes seen in these action selection task experiments.

Finally, the application of low and high frequency DBS was used to see if the β-band increases in the first case, what could be an explanation for the worsen of the PD patients which receive these frequencies, and decreases in the second, what could show the improvement of the patients. Results showed the expected behavior, increasing significantly the β-band for low frequency DBS (around 6 times) and decreasing for high frequency (smaller but near healthy values), indicating that β-band could be considered a good option to be used as biomarker for proper high frequency DBS treatment.

6. References

[1] W. Poewe *et al.*, "Parkinson disease," *Nat. Rev. Dis. Prim.*, vol. 3, p. 17013, Mar. 2017.

[2] J. M. Beitz, "Parkinson's disease: a review," *Front Biosci*, vol. 6, no. 6574.31, 2014.

[3] D. Twelves, K. S. M. Perkins, and C. Counsell, "Systematic review of incidence studies of Parkinson's disease," *Mov. Disord.*, vol. 18, no. 1, pp. 19–31, Jan. 2003.

[4] S. K. Van Den Eeden *et al.*, "Incidence of Parkinson's disease: variation by age, gender, and race/ethnicity," *Am. J. Epidemiol.*, vol. 157, no. 11, pp. 1015–1022, 2003.

[5] M. Kusumi, K. Nakashima, H. Harada, H. Nakayama, and K. Takahashi, "Epidemiology of Parkinson's disease in Yonago City, Japan: comparison with a study carried out 12 years ago," *Neuroepidemiology*, vol. 15, no. 4, pp. 201–207, 1996.

[6] J. M. Fearnley and A. J. Lees, "Ageing and Parkinson's disease: substantia nigra regional selectivity," *Brain*, vol. 114, no. 5, pp. 2283–2301, 1991.

[7] P. Damier, E. C. Hirsch, Y. Agid, and A. M. Graybiel, "The substantia nigra of the human brain: II. Patterns of loss of dopamine-containing neurons in Parkinson's disease," *Brain*, vol. 122, no. 8, pp. 1437–1448, 1999.

[8] H. Braak, K. Del Tredici, U. Rüb, R. A. I. De Vos, E. N. H. J. Steur, and E. Braak, "Staging of brain pathology related to sporadic Parkinson's disease," *Neurobiol. Aging*, vol. 24, no. 2, pp. 197–211, 2003.

[9] K. R. Chaudhuri and A. H. V Schapira, "Non-motor symptoms of Parkinson's disease: dopaminergic pathophysiology and treatment," *Lancet Neurol.*, vol. 8, no. 5, pp. 464–474, 2009.

[10] M. A. Hely, W. G. J. Reid, M. A. Adena, G. M. Halliday, and J. G. L. Morris, "The Sydney multicenter study of Parkinson's disease: the inevitability of dementia at 20 years," *Mov. Disord.*, vol. 23, no. 6, pp. 837–844, 2008.

[11] G. E. Alexander, M. D. Crutcher, and M. R. DeLong, "Basal ganglia-thalamocortical circuits: parallel substrates for motor, oculomotor, 'prefrontal' and 'limbic' functions," in *Progress in brain research*, vol. 85, Elsevier, 1991, pp. 119–146.

[12] G. E. Alexander, M. R. DeLong, and P. L. Strick, "Parallel organization of functionally segregated circuits linking basal ganglia and cortex," *Annu. Rev. Neurosci.*, vol. 9, no. 1, pp. 357–381, 1986.

[13] A. Nambu, H. Tokuno, and M. Takada, "Functional significance of the cortico-subthalamo–pallidal 'hyperdirect' pathway," *Neurosci. Res.*, vol. 43, no. 2, pp. 111–117, 2002.

[14] C. Baston and M. Ursino, "A Biologically Inspired Computational Model of Basal Ganglia in Action Selection," *Comput. Intell. Neurosci.*, vol. 2015, pp. 1–24, 2015.

[15] H. Schroll and F. H. Hamker, "Computational models of basal-ganglia pathway functions: focus on functional neuroanatomy," *Front. Syst. Neurosci.*, vol. 7, no. December, pp. 1–18, 2013.

[16] R. Moroney, C. Heida, and J. Geelen, "Increased bradykinesia in Parkinson's disease with increased movement complexity: Elbow flexion - Extension movements," *J. Comput. Neurosci.*, vol. 25, no. 3, pp. 501–519, 2008.

[17] M. J. Frank, J. Samanta, A. A. Moustafa, and S. J. Sherman, "Hold your horses: impulsivity, deep brain stimulation, and medication in parkinsonism," *Science (80- .).*, vol. 318, no. 5854, pp. 1309–1312, 2007.

[18] A. A. Kühn *et al.*, "Event-related beta desynchronization in human subthalamic nucleus correlates with motor performance," *Brain*, vol. 127, no. 4, pp. 735–746, 2004.

[19] P. Brown, "Abnormal oscillatory synchronisation in the motor system leads to impaired movement," *Curr. Opin. Neurobiol.*, vol. 17, no. 6, pp. 656–664, 2007.

[20] M. D. Humphries, J. A. Obeso, and J. K. Dreyer, "Insights into Parkinson's disease from computational models of the basal ganglia," *J. Neurol. Neurosurg. Psychiatry*, pp. 1181–1188, 2018.

[21] S. Ahn, S. E. Zauber, R. M. Worth, and L. L. Rubchinsky, "Synchronized Beta-Band Oscillations in a Model of the Globus Pallidus-Subthalamic Nucleus Network under External Input," *Front. Comput. Neurosci.*, vol. 10, no. December, pp. 1–12, 2016.

[22] S. Gauggel, M. Rieger, and T. A. Feghoff, "Inhibition of ongoing responses in patients with Parkinson's disease," *J. Neurol. Neurosurg. Psychiatry*, vol. 75, no. 4, pp. 539–544, 2004.

[23] J. A. Cooper, H. J. Sagar, P. Tidswell, and N. Jordan, "Slowed central processing in simple and go/no-go reaction time tasks in parkinson's disease," *Brain*, vol. 117, no. 3, pp. 517–529, 1994.

[24] B. Pasquereau and R. S. Turner, "A selective role for ventromedial subthalamic nucleus in inhibitory control," *Elife*, vol. 6, pp. 1–27, 2017.

[25] D. Benis *et al.*, "Subthalamic nucleus activity dissociates proactive and reactive inhibition in patients with Parkinson's disease," *Neuroimage*, vol. 91, pp. 273–281, 2014.

[26] T. Otsuka, T. Abe, T. Tsukagawa, and W.-J. Song, "Conductance-Based Model of the Voltage-Dependent Generation of a Plateau Potential in Subthalamic Neurons," *J. Neurophysiol.*, vol. 92, no. 1, pp. 255–264, 2004.

[27] D. Terman, J. E. Rubin, A. C. Yew, and C. J. Wilson, "Activity Patterns in a Model for the Subthalamopallidal Network of the Basal Ganglia," *J. Neurosci.*, vol. 22, no. 7, pp. 2963–2976, 2002.

[28] C. Park, R. M. Worth, and L. L. Rubchinsky, "Neural dynamics in Parkinsonian brain: The boundary between synchronized and nonsynchronized dynamics," *Phys. Rev. E - Stat. Nonlinear, Soft Matter Phys.*, vol. 83, no. 4, pp. 1–4, 2011.

[29] A. J. Nevado-Holgado, N. Mallet, P. J. Magill, and R. Bogacz, "Effective connectivity of the subthalamic nucleus-globus pallidus network during Parkinsonian oscillations," *J. Physiol.*, vol. 592, no. 7, pp. 1429–1455, 2014.

[30] M. Jahanshahi, I. Obeso, C. Baunez, M. Alegre, and P. Krack, "Parkinson's disease, the subthalamic nucleus, inhibition, and impulsivity," *Mov. Disord.*, vol. 30, no. 2, pp. 128–140, 2015.

[31] J. E. Rubin, "Computational models of basal ganglia dysfunction: the dynamics is in the details," *Curr. Opin. Neurobiol.*, vol. 46, no. Dd, pp. 127–135, 2017.

[32] K. T. Zitelli, T. C. Whalen, S. Y. Crilly, V. L. Corbit, A. H. Gittis, and J. E. Rubin, "Pallidostriatal Projections Promote Oscillations in a Dopamine-Depleted Biophysical Network Model," *J. Neurosci.*, vol. 36, no. 20, pp. 5556–5571, 2016.

[33] J. E. Rubin and D. Terman, "High Frequency Stimulation of the Subthalamic Nucleus Eliminates ...," pp. 211–235, 2004.

[34] A. Pavlides, S. J. Hogan, and R. Bogacz, "Computational Models Describing Possible Mechanisms for Generation of Excessive Beta Oscillations in Parkinson's Disease," *PLoS Comput. Biol.*, vol. 11, no. 12, pp. 1–29, 2015.

[35] P. Limousin *et al.*, "Bilateral subthalamic nucleus stimulation for severe Parkinson's disease," *Mov. Disord. Off. J. Mov. Disord. Soc.*, vol. 10, no. 5, pp.

672–674, 1995.

[36] G. Scheler, "Learning intrinsic excitability in medium spiny neurons," *F1000Research*, vol. 2, no. May, p. 88, 2014.

[37] S. Mahon, J. M. Deniau, S. Charpier, and B. Delord, "Role of a striatal slowly inactivating potassium current in short-term facilitation of corticostriatal inputs: A computer simulation study," *Learn. Mem.*, vol. 7, no. 5, pp. 357–362, 2000.

[38] K. Du *et al.*, "Cell-type – specific inhibition of the dendritic plateau potential in striatal spiny projection neurons," 2017.

[39] A. J. Gruber *et al.*, "Modulation of Striatal Single Units by Expected Reward : A Spiny Neuron Model Displaying Dopamine-Induced Bistability," pp. 1095–1114, 2003.

[40] K. M. Biddell and J. D. Johnson, "A biophysical model of cortical glutamate excitation of medium spiny neurons in the dorsal lateral striatum," in *2013 IEEE 56th International Midwest Symposium on Circuits and Systems (MWSCAS)*, 2013, pp. 964–966.

[41] S. Damodaran, X. J. R. Cressman, X. Z. Jedrzejewski-szmek, and X. K. T. Blackwell, "Desynchronization of Fast-Spiking Interneurons Reduces □ -Band Oscillations and Imbalance in Firing in the Dopamine-Depleted Striatum," vol. 35, no. 3, pp. 1149–1159, 2015.

[42] S. J. Cragg, J. Baufreton, Y. Xue, J. P. Bolam, and M. D. Bevan, "Synaptic release of dopamine in the subthalamic nucleus," *Eur. J. Neurosci.*, vol. 20, no. 7, pp. 1788–1802, 2004.

[43] D. S. Kreiss, C. W. Mastropietro, S. S. Rawji, and J. R. Walters, "The Response of Subthalamic Nucleus Neurons to Dopamine Receptor Stimulation in a Rodent Model of Parkinson's Disease," *J. Neurosci.*, vol. 17, no. 17, pp. 6807–6819, 2018.

[44] A. Galvan *et al.*, "Localization and function of dopamine receptors in the subthalamic nucleus of normal and parkinsonian monkeys," *J. Neurophysiol.*, vol. 112, no. 2, pp. 467–479, 2014.

[45] H. Parasuram, B. Nair, E. D'Angelo, M. Hines, G. Naldi, and S. Diwakar, "Computational Modeling of Single Neuron Extracellular Electric Potentials and Network Local Field Potentials using LFPsim," *Front. Comput. Neurosci.*, vol. 10, no. June, pp. 1–13, 2016.

[46] A. Mazzoni, H. Lindén, H. Cuntz, A. Lansner, S. Panzeri, and G. T. Einevoll, "Computing the Local Field Potential (LFP) from Integrate-and-Fire Network Models," *PLoS Comput. Biol.*, vol. 11, no. 12, pp. 1–38, 2015.

[47] H. J. Lee *et al.*, "Activation of Direct and Indirect Pathway Medium Spiny Neurons Drives Distinct Brain-wide Responses Article Activation of Direct and Indirect Pathway Medium Spiny Neurons Drives Distinct Brain-wide Responses," *Neuron*, vol. 91, no. 2, pp. 412–424, 2016.

[48] T. V. Wiecki and M. J. Frank, "A computational model of inhibitory control in frontal cortex and basal ganglia," *Psychol. Rev.*, vol. 120, no. 2, pp. 329–355, 2013.

[49] M. J. Frank, "Hold your horses: A dynamic computational role for the subthalamic nucleus in decision making," *Neural Networks*, vol. 19, no. 8, pp. 1120–1136, 2006.

[50] S. Stuart, R. Vitorio, R. Morris, D. N. Martini, P. C. Fino, and M. Mancini, "and Parkinson ' s disease : a structured review," pp. 53–72, 2019.

[51] M. M. Mcgregor and A. B. Nelson, "Review Circuit Mechanisms of Parkinson ' s Disease," *Neuron*, vol. 101, no. 6, pp. 1042–1056, 2019.

[52] O. Monchi, M. Petrides, B. Mejia-constain, and A. P. Strafella, "Cortical activity in Parkinson ' s disease during executive processing depends on striatal

involvement," vol. 130, no. Pt 1, pp. 233–244, 2013.

Appendix

This appendix includes the values of the parameters used for the different populations of neurons. Also, values corresponding to the parkinsonian states and the parameters of the simulated functions that are not mentioned in the report are included.

Table 1. Values of the electrophysiological parameters of the different populations of neurons.

Parameter	MSN Go part	MSN No-Go part	FSI	GPe	STN	GPi	Thalamus
g_{L}	0.075	0.04	0.25	0.1	2.25	0.1	0.05
g_{K}	6	6	112.5	30	45	30	30
g_{Na}	35	35	56.25	120	37.5	120	120
g_{Ca}	0.1	0.1	-	0.15	0.5	0.15	-
g_{T}	-	-	-	0.5	0.5	0.5	0.5
g_{AHP}	-	-	-	30	9	30	-
E_{L}	-65	-65	-70	-55	-60	-55	-60
E_{K}	-90	-90	-90	-80	-80	-80	-90
E_{Na}	55	55	50	55	55	55	50
E_{Ca}	140	140	-	120	140	120	0
τ_{h}^{0}	0.5	0.5	0.5	0.05	1	0.05	-
τ_{h}^{1}	110.1	30.1	25	0.27	500	0.27	-
τ_{n}^{0}	0.5	0.5	0.5	0.05	1	0.05	-
τ_{n}^{1}	110	30	25.4	0.27	100	0.27	-
τ_{r}^{0}	-	-	-	30	7.1	30	-
τ_{r}^{1}	-	-	-	0	17.5	0	-
Φ_{h}	1	1	1	0.05	0.75	0.05	-
Φ_{n}	1	1	1	0.1	0.75	0.1	-
Φ_{r}	-	-	-	1	0.5	1	-
k_{l}	-	-	-	30	15	30	-
k_{Ca}	-	-	-	15	22.5	15	-
ϵ	-	-	-	5e-4	5e-5	5e-4	-
θ_{m}	-38	-38	-44	-37	-30	-37	-37
θ_{h}	-58	-58	-58.3	-58	-39	-58	-41
θ_{n}	-47	-47	-42.4	-50	-32	-50	-
θ_{r}	-	-	-	-70	-67	-70	-84
θ_{a}	-	-	-	-57	-63	-57	-60
θ_{b}	-	-	-	-	0.25	-	-
θ_{s}	-37	-37	-	-35	-39	-35	-
$\theta_{\mathrm{h}}^{\tau}$	-43.5	-43.5	-12	-40	-57	-40	-
$\theta_{\mathrm{n}}^{\tau}$	-37.4	-37.4	-8.6	-40	-80	-40	-
$\theta_{\mathrm{r}}^{\tau}$	-	-	-	-	68	-	-
$\theta_{\mathrm{g}}^{\mathrm{H}}$	-57.8	-57.8	-57.8	-57	-39	-57	-
θ_{g}	52	52	57	20	8	20	-
σ_{m}	10	10	11.5	10	15	10	7
σ_{h}	-20	-20	-6.7	-12	-3.1	-12	-6
σ_{n}	14	14	6.8	14	8	14	-
σ_{r}	-	-	-	-2	-2	-2	4
σ_{a}	-	-	-	2	7.8	2	6.2
σ_{b}	-	-	-	-	-0.07	-	-
σ_{s}	2	2	-	2	8	2	-
$\sigma_{\mathrm{h}}^{\tau}$	-12.63	-12.63	-60	-12.1	-3	-12.1	-
$\sigma_{\mathrm{n}}^{\tau}$	-12.3	-12.3	-14.6	-12	-26	-12	-
$\sigma_{\mathrm{r}}^{\tau}$	-	-	-	-	-2.2	-	-
$\sigma_{\mathrm{g}}^{\mathrm{H}}$	2	2	2	2	8	2	-

α	2	2	2	2	5	2	-
β	0.1	0.1	0.2	0.08	1	0.08	-

With respect to the conductivities and resting potential of the different connections between networks, the values are defined as:

Table 2. Values of the parameters of connectivity
between the different populations.

Connection	$g_{A \to B}$	$E_{A \to B}$
MSN → MSN (No-Go part)	0.5	-80
MSN → GPe (healthy)	0.3	-80
FSI → MSN	0.1	-80
MSN → MSN (Go part)	0.14	-80
MSN → GPi (healthy)	0.6	-80
FSI → FSI	0.3	-80
GPe → FSI	0.12	-80
GPe → GPe	0.01	-100
STN → GPe	0.3	0
GPe → STN	0.4	-100
STN → GPi	0.3	0
GPi → Thalamus	0.05	-85
MSN → GPe (mild PD)	0.55	-80
MSN → GPi (mild PD)	0.455	-80
STN → GPe (mild PD)	0.275	0
STN → GPi (mild PD)	0.275	0
MSN → GPe (severe PD)	1.3	-80
MSN → GPi (severe PD)	0.02	-80
STN → GPe (severe PD)	0.2	0
STN → GPi (severe PD)	0.2	0

Finally, with respect to the input signals used for the action selection task, the most optimal outcome as stated in Methods was for frequency of 80Hz and amplitude of 200, in both cases.